UNIVERSITÀ DEGLI STUDI DI MILANO

FACOLTÀ DI MEDICINA E CHIRURGIA

DIPARTIMENTO DI MORFOLOGIA UMANA E SCIENZE BIOMEDICHE
CITTA' STUDI

CORSO DI DOTTORATO DI RICERCA IN
SCIENZE MORFOLOGICHE CICLO XXIV

TESI DI DOTTORATO DI RICERCA

PRECLINICAL TESTING OF GALECTIN-3C FOR MULTIPLE MYELOMA

BIO16

Dr. Maurizio Chiriva Internati
Matr. R08106

TUTOR Chiar.ma Prof.ssa Isabella Barajon

COORDINATORE DEL DOTTORATO Chiar.ma Prof.ssa Laura Vizzotto

ANNO ACCADEMICO 2011/2012

CONTENTS

SUMMARY

The American Cancer Society expects that there will be more than 20,000 new cases of multiple myeloma (MM) in the US in 2011 and despite the new treatments now available, the median survival rate is only 5 years. Galectin-3C (Gal-3C) is a human lectin involved in cellular processes including cellular differentiation, apoptosis, neoplastic transformation, and metastasis. Gal-3C contains the carbohydrate recognition domain (CRD) of galectin-3 and is thought to act as a dominant negative inhibitor of galectin-3-mediated cross-linking. Gal-3C is a proprietary truncated, inhibitory form of galectin-3. Results showed that in a subcutaneous U266 cell NOD/SCID mouse model of human MM, treatment with an *N*-terminally truncated form of galectin-3, termed Gal-3C significantly inhibited tumor growth. Furthermore, *in vitro* data indicated that Gal-3C acts by inhibition of angiogenesis, MM cell migration and invasion, and NF-kB activation. Moreover, Gal-3C facilitates the antitumor activity of bortezomib, a proteasome inhibitor for MM treatment. Gal-3C and bortezomib also synergistically inhibited MM-induced angiogenesis activity *in vitro*. The delivery of Gal-3C to patients will be via a pump during initial clinical trials. In the long-term, the plan is to develop a formulation of Gal-3C for sustained release to increase survival for patients with MM.

ABBREVIATIONS

AAV: adeno-associated virus
AHSC: autologous hematopoietic stem cell
AKAP-4: A-kinase anchor proteins-4
ANOVA: analysis of variance
B cell: bone cell
B2m: b2-microglobulin
BAFF/APRIL: B-cell activating factor/proliferation inducing ligand
BCL-2: B-cell lymphoma 2
bFGF: basic fibroblast growth factor
BM: bone marrow
BOR: bortezomib
BSA: bovine serum albumin
CC: chemokine
CD138: cluster differentiation 138
cDNA: complementary deoxyribonucleic acid
CM: conditioned medium
CO_2: carbon dioxide
CRD: carbohydrate recognition domain
CTA: cancer testis antigens
CTL: cytotoxic T lymphocyte
CXCR4: C-X-C chemokine receptor type 4
DEX: dexamethasone
DLBCL: diffuse large B-cell lymphoma
DNA: deoxyribonucleic acid
DNase: deoxyribonuclease enzyme
EBM-2: endothelial cell basal medium-2
EGM-2: endothelial cell growth medium-2
ELISA: enzyme-linked immunosorbent assay
EXC: chemokine receptor
FACs: cytofluorimetric analysis
FBS: fetal bovine serum
FDA: food and drug administration
Gal-3C: galectin 3C
GFP: green fluoresce protein
HUVEC: human umbilical cord vascular endothelial cells
IF: immunofluorescence
Ig: immunoglobulin
IHC: immunohistochemistry
IKBα: nuclear factor of kappa light
IKK: Inhibitor of nuclear factor kappa-kinase
IL: interleukin
IL-6: interleukin 6
IL-2: interleukin 2
mAbs: mouse antibodies
MGUS: monoclonal gammapathy of unknown significance
MM: multiple myeloma

MMPs: metalloproteinases
M-PER: protein extraction buffer
NCI: national cancer institute
NF-KB: nuclear factor -kappa-B
NIH: national institutes of health
NK: natural killer
NOD/SCID: non-obese diabetic /severe combined immunodeficient
PBS: phosphate-buffered saline
PC: plasma cell
PCR: polymerase chain reaction
PEL: primary effusion lymphoma
PFA: paraformaldehyde fixation buffer
PSA: prostate antigen specific
RANTES: regulated on activation, normal T expressed and secreted
RHAMM: hyaluronan-mediated motility receptor
RNA: ribonucleic acid
RPMI: Roswell Park Memorial Institute medium
RT-PCR: reverse transcription polymerase chain reaction
RT: room temperature
SDF-1a: stromal-cell derived factor-1 alpha
SDS-PAGE: sodium dodecyl sulfate polyacrylamide gel electrophoresis
SC: subcutaneous
TGFb: transforming growth factor beta
THAL: thalidomide
TMB: tetramethylbenzidine
TNFa: tumor necrosis factor alpha
USA: United States of America
VCAM-1: vascular cell adhesion molecule 1
VEGF: vascular endothelial growth factor
VTE: venous thromboembolism
WnT: proto-oncogene protein

1. INTRODUCTION

1.1 MULTIPLE MYELOMA

Multiple myeloma (MM) is a malignancy caused by clonal proliferation and accumulation of terminally differentiated B plasma cells (PCs) that accumulate in the bone tissue, causing bone destruction and interference with normal PC activity by altered PCs that generate non-specific monoclonal Igs called the "M-protein" [1].

MM is always preceded by a premalignant stage called monoclonal gammopathy of unknown significance (MGUS) [2]. Initially, MM is a slowly proliferating tumor. Less than 1% of MM cells synthesize DNA until the very late stages of the disease [3] when the cells are found outside the bone marrow (BM) in extramedullary locations including peripheral blood, pleural effusion, and ascites [4]. MM inevitably spreads to involve the entire BM causing death.

MM symptoms include dysregulation of calcium, renal failure, anemia, and bone lesions. MM is diagnosed by blood and urine tests, and in advanced disease skeletal surveys are used for bone assessment. A staging system is based on serum levels of calcium, creatinine, hemoglobin, M-protein, and most significantly, serum albumin and b2-microglobulin (b2m). Median survival in stage I is 62 months, in stages II and III, 45 and 29 months, respectively [5,6].

The development of cytogenetic, genomic, and proteomic markers for MM [7-15] are expected to lead to new targeted therapeutics and rational drug combinations.

Chemotherapy induces complete tumor regression in ~50% of patients [16]. The introduction of novel drugs has aided in the treatment of MM especially in management of elderly patients [3, 9], and has improved survival rates [17], but the eventual outcome is relapse and chemoresistant

disease. The median age at diagnosis is 69 years for men and 72 years for women (rarely occurring before 40) and the median survival is only 5 years [17]. Current chemotherapy induces complete tumor regression in about 50% of patients [3, 9]. However, outcome from the frontline treatment for MM, autologous hematopoietic stem cell (AHSC) transplant, is usually favorable only in younger patients where it increases the rate of complete remission and prolongs event-free survival compared with conventional chemotherapy [17].

Pharmacologic interventions are the only option for the majority of patients who are older. A MM cure is viewed as distant, but further improvements in survival time are considered achievable [16].

The introduction of novel drugs such as thalidomide, lenalidomide, and bortezomib (Bor) that are thought to target specific intracellular pathways and affect cellular interactions with the tumor microenvironment, has aided in the treatment of MM, especially in the management of elderly patients [19].

In the last several years, interesting information into the molecular mechanisms of the development of MM was achieved for successful therapeutics, such as proteasome inhibitors [20].

Bor, a boronic acid dipeptide, was the first-in-class proteasome inhibitor approved by the US Food and Drug Administration (FDA) for the treatment of relapsed and refractory MM [20, 21]. Deregulation of the ubiquitin-proteasome signaling pathway is linked to the etiology of various human diseases; therefore, proteasome inhibitors offer great promise as therapeutic agents [20, 21].

1.2 DRUGS IN MULTIPLE MYELOMA

Dexamethasone (DEX) is a synthetic element of the glucocorticoid class of steroid. This drug has been used as an anti-inflammatory and immunosuppressant. DEX is more potent than the hormones, cortisol and prednisone.

DEX was used to treat autoimmune conditions, rheumatoid arthritis and other different conditions such as brochospasms, and DEX has been used to fight allergic anaphylactic shock. Furthermore, DEX has been used as a chemotherapeutic agent in MM and as an adjuvant in other cancers to combat some of the side effects of chemotherapy.

The side effects of DEX are stomach distress, increased stomach ulcers, diabetes mellitus, personality changes, osteoporosis, muscle atrophy, and acne. This glucocorticoid steroid is excreted mainly in the urine and has a half-life of 36-54 h [15-21].

Thalidomide (THAL) is an immunomodulatory agent (dioxopiperidin) developed by German pharmaceutical company in the 50's as a possible antidote to nerve toxins and sedative drug to combat morning sickness. It was withdrawn in 1961 due to tetragenicity and neuropathies.

From 1957 to 1961, this drug caused more than 10,000 birth defects in more the 40 countries. The side effects of this drug led to more restricted testing before future drug licensing.

In 1994, Dr. Robert D'Amato at Harvard Medical School discovered that thalidomide is a potent inhibitor of anti-angiogenic effects.

THAL use in MM appears to slow down the progression of the disease by halting the production of interleukin-6 (IL-6), a key player in the proliferation of MM cells. Furthermore, it activates apoptotic pathways and T cells to produce interleukine-2 (IL-2), increasing the

activity of natural killer (NK) cells [15-21, 80. This drug has several side effects such as polyneuropathy, fatigue, skin rash, venous thromboembolism (VTE), stroke, and myocardial infarction.

THAL is metabolized *in vivo* and metabolites are excreted primarily in the urine. The half-life is in the order of a few hours [17-29, 80].

Bortezomib (BOR) was originated in 1995 and was originally called MG-341 by ProScript. This dug is an N-protected dipeptide (phenylalanine and leucine) with boronic acid [21-29, 77, 80-82]. The mechanism of this drug is based on the boron atom in bortezomib which binds the catalytic site of the proteosome (26S).

The proteosome in the normal cells regulates protein expression and function by eliminating cells that misfolded proteins. This mechanism is extremely important in maintaining cell immortality [21-29, 77, 80-82]. This drug reaches its peak in about 30 minutes. BOR levels have been measured by proteosome inhibition in peripheral blood mononuclear cells (PBMC). This small molecule is the first proteosome inhibitor to be used in humans [21-29, 77, 80-82].

Side effects of this drug are the following: peripheral neuropathy, myelosuppression, neutropenia, thrombocytopenia, shingles, gastro-intestinal distress and asthenia. This anticancer agent has a half-life of 8 to 15 h.

1.3 MULTIPLE MYELOMA TARGETED THERAPIES AND TUMOR MICROINVIROMENTS

Figure 1 describes how to prevent drug resistance and improve patient outcome by simultaneously targeting MM cells and their microenvironment in the BM [13, 14, 22, 24, 31]. Adhesion to BM stromal cells is thought to prevent apoptosis, affect transcriptional diversity, differentiation of MM cells, and secretion of cytokines, such as IL-6, that promote MM cell growth, survival and migration [21-24], and also blocks apoptosis [21-24].

Many anticancer agents trigger apoptosis that precedes via common downstream effector pathways [21-24], and Bor inhibits the proteasome which functions like a “garbage disposal," removing abnormal or damaged proteins. Bor causes proteins to accumulate including BAX that facilitates apoptosis by blocking Bcl-2. Major cell surface receptors for BM extracellular matrix components on MM cells include integrins and the stromal cell, VCAM-1.

Molecules such as CD44 isoforms, RHAMM, and CD38 are thought to mediate interactions of MM cells with hyaluronan. CXCR4 is an MM cell receptor for stromal-cell derived factor-1 alpha (SDF-1a) that facilitates adhesion and signals BM homing. Adhesion of MM to BM has been targeted in the development of new agents [21-25, 81, 82] such as mAbs to syndecan-1 (CD138; a heparin sulfate proteoglycan), and lotuzumab, that binds a cell surface glycoprotein, CS-1, found on MM cells [20-29, 30-33].

FIGURE 1

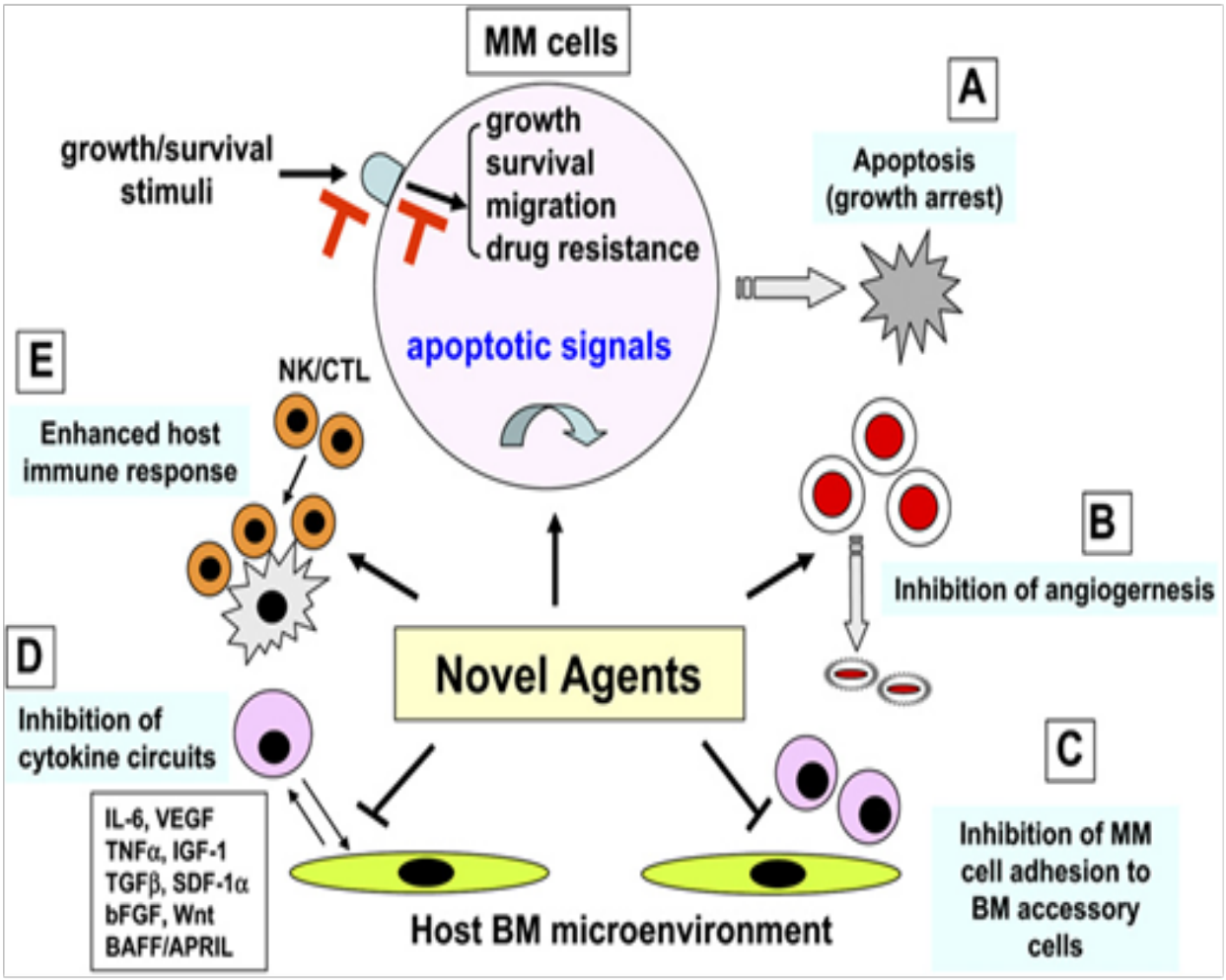

Fig. 1 *Novel agents targeting MM and the BM microenvironment (A) cause apoptosis or growth arrest, inhibit (B) angiogenesis, (C) MM cell adhesion to BM cells, and (D) cytokine production, or (E) enhance host anti-MM immunity. From Hideshima & Anderson (2007).*

1.4 GALECTIN

Galectin-3 is a member of the galectin family of animal lectins that is defined based on sequence homology within the carbohydrate recognition domain (CRD) and a characteristic affinity for b-galactosides (see fig. 2) [25-27]. The amino-terminal domain is critical for the multivalent behavior.

Alone the carboxy-terminal CRD lacks hemagglutination activity and the cooperative binding [28-29]. The amino-terminus enables the CRD to cross-link carbohydrate-containing ligands on cell surfaces and in the extracellular matrix and, thus, to modulate cell adhesion and signaling [27-31].

Galectin-3 has been found to be involved in multiple cellular processes. Key roles of galectin-3 in the regulation of the adhesive properties of metastatic cancer cells, and invasive potentials were originally elucidated in pioneering work by Raz *et al.* [32]. Lectins including the galectin family [32] have gained increasing recognition as potential therapeutic targets [25-27, 33-36], and specific associations of the expression of galectin-3 with cell growth, neoplastic transformation, apoptosis, and metastasis have been reported [25-27, 37-38]. In

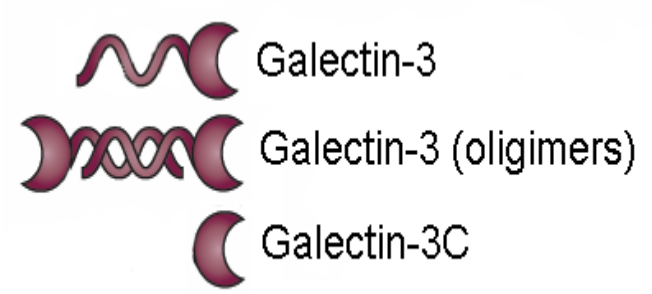

Fig. 2 *Galectin-3 (**top**) with CRD to right and N-terminal domain (left). Galectin-3 molecules (**middle**) homodimerized through the N-terminal domains. Gal-3C (**bottom**) retains carbohydrate binding but does not form multimers.*

prostate cancer, a small clinical trial of modified citrus pectin, a natural product thought to inhibit galectin-3, produced greater doubling times for prostate specific antigen (PSA) levels, and the only apparent side effect was abdominal discomfort [47].

Galectin-3 is thought to participate in regulation of the inflammatory state of various immune cells. Several studies indicate that it plays a novel regulatory role in the B cell compartment [35-41] including PCs [41].

Hoyer *et al.* found stage-specific expression during B-cell development [35-43]. Increased galectin-3 levels were observed in some of the neoplasms that derive from these cells, specifically diffuse large B-cell lymphoma (DLBCL), primary effusion lymphoma (PEL), and MM [39-43].

Tumor growth and metastasis were virtually eliminated in mice lacking Mgat5, an enzyme forming antenna-like oligosaccharides containing lactosamines [43] on molecules such as fibronectin recognized by galectin-3 [39-44]. Several tumor antigens express high levels of lactosamines, and the affinity of galectin-3 for lactosaminylated oligosaccharides is higher than that of most galectins [39-45].

Silencing expression of galectin-3 in animal models of human cancers including prostate [39-47, 57] and breast cancers, reduced tumor growth and metastasis.

Apparently contradictory results were obtained when galectin-3(-/-) mutant mice were crossed with genetic mouse models of intestinal cancer, Apc^{Min} and Apc^{1638N}, and a mouse mammary gland model, *PyMT*. Galectin-3 was *not* a rate-limiting factor in tumorigenicity in these mice [44-46]. This likely was due to activity of other members of the galectin family, and the more than 1.3 fold up- or down-regulation of the expression of 22 glycosyltransferases [48,49].

Gal-3C consists of the 143 carboxy-terminal a.a. residues of human galectin-3. Gal-3C retains carbohydrate binding but lacks the *N*-terminal domain (Fig. 2), and acts as a dominant negative

inhibitor competing with endogenous galectin-3 for carbohydrate binding sites and preventing its homodimeric cross-linking [50]. Subsequently, the study by Hoyer *et al.*, showed that overexpression of Gal-3C in galectin-3-expressing primary effusion lymphoma cells facilitated Fas-mediated apoptosis, whereas galectin-3 overexpression in galectin-3-negative Burkitt lymphoma cells inhibited Fas-mediated apoptosis [49,50].

2. AIM OF THE STUDY

The main hypothesis for this study is to evaluate the potential of Gal-3C, an N-terminally truncated form of galectin-3 that is thought to act as a dominant negative inhibitor, for the treatment of multiple myeloma (MM).

3. RESEARCH DESIGN AND METHODS

3.1 Experimental Design.

These *in vitro* and *in vivo* models investigated the presence of Galectin 3C expression in 9 human MM cell lines and the capacity of Galectin 3C to inhibit proliferation of these MM cell lines. In addition, the capacity of Galectin 3C inhibition of chemotaxis of the U266 MM cell line was tested.

An adeno-associated virus (AAV) and green fluorescence protein (GFP) AAV/GFP virus stock was generated and tested to infect the U266 cell line. The infection was confirmed by immunofluorescence (IF) labeling, (RT-PCR) and cytofluorimetric analysis (FACs). The single components of Bortezomib and Galectin 3C, singularly were tested, and the combination of both in the U266 MM mouse model non-obese diabetic /severe combined immunodeficiency (NOD/SCID). The results were analyzed by immunohistochemistry (IHC), RT-PCR, Enzyme-Linked Immunosorbent Assay (ELISA) and Dot Blot. The tumor expression was tested by

human immunoglobulin (Ig) IgE, Igλ and A-kinase anchor proteins-4 (AKAP-4) [73]. Further, the synergistic effects of Bortezomib and Gal-3C were tested for their ability to inhibit endothelial cell migration and angiogenesis. Moreover, flow-cytometry analysis was used to observe if Gal-3C impaired nuclear factor-kappa-B (NF-KB) activation induced by Bortezomib in U266 [58].

3.2 Animals

Six-week-old female NOD.CB17-Prkdcscid/J (NOD/SCID) mice [72] purchased from the Jackson Laboratory (Bar Harbor, ME, USA) were used. Treatment and care were in accordance with the Institutional Guidelines and the Animal Welfare Assurance Act. [51,72].

3.3 Cells and media.

Human MM cell lines RPMI-8226, U266 (American Type Culture Collection, VA, USA), ARP-1, ARK-B, (gifts from J. Epstein, University of Arkansas for Medical Sciences, Little Rock, AR, USA) were used. The MM cell lines MM.1S and MM.1RL were generously provided by Dr. Steven T. Rosen (Northwestern University, Evanston, IL, USA) and the NCI-H929 cell line was donated by Dr. Steven D. Rosen (University of California, San Francisco, CA, USA). The 8226/Dox and 8226/LR-5 cell lines were kindly provided by Dr. William S. Dalton of the H. Lee Moffitt Cancer Center and Research Institute (Tampa, FL, USA). All MM cells were cultured in Roswell Park Memorial Institute medium-1640 (RPMI-1640 medium), and supplemented with 10% fetal bovine serum (FBS) in 5% CO2 at 37°C. The 8226/Dox cells were cultured with 40 nM doxorubicin (Sigma-Aldrich, St. Louis, MO, USA). The 8226/LR-5 cells were cultured in media containing 5 mM mephalan (Sigma-Aldrich). 8226/Dox and 8226/LR-5 cells were maintained in drug-free medium for 1 week prior to drug sensitivity assays.

Human umbilical cord vascular endothelial cells (HUVEC), (American Type Culture Collection, VA, USA) were maintained in Endothelial Cell Growth Medium (EGM-2 medium) (Lonza, Houston, TX, USA) and were used within 10 sub-culturing passages [72].

3.4 SDS-PAGE and Immunoblot.

Flasks of MM cells were harvested, lysed by freezing, and the proteins extracted with M-PER protein buffer (Thermo, Rockford, IL) using Protease Inhibitor Cocktail (Sigma-Aldrich). Protein concentration was determined with the Bio-Rad Protein Assay (Hercules, CA), and equal amounts of each sample were resolved by 4-12% Bis-Tris PAGE (Invitrogen) after heating (70°C, 10 min) in sample buffer.

Proteins were electrotransferred onto nitrocellulose, efficiency confirmed by reversible staining with Ponceau S (Sigma-Aldrich), and the blot incubated with anti-galectin-3 antibody [72] (M3/38, Santa Cruz Biotechnology, Santa Cruz, CA), followed by biotin-conjugated anti-rat IgG, horseradish peroxidase (HRP)-conjugated streptavidin, and then TMB with membrane enhancer (KPL; Mandel, Guelph, Canada)[72]. Pictures were taken with a digital camera [72].

3.5 Drugs and mini-pumps.

Bortezomib (Bor) was acquired from Millennium Pharmaceuticals (Cambridge, MA, USA). Gal-3C was used as previously described [72]. Doxorubicin and mephalan were purchased from Sigma-Aldrich (St.Louis, MO, USA). The 200 ml mini-osmotic pumps are specifically built to deliver 0.5 mL/h were purchased from DURECT Corporation (Cupertino, CA, USA) [72].

3.6 Cell proliferation assays.

Cell proliferation was assessed by quantification of ATP metabolism by viable cells (ViaLight Plus, Lonza, Walkersville, MD). In brief, myeloma cells were seeded (8,000 per well) in growth media and, while HUVEC cells were seeded (10,000/well) in 50ml EGM-2 in 96 well plates. The proliferation assay was assessed after 48 h. Aliquots of Gal-3C (dialyzed to remove lactose), thalidomide, Dex, Bor, doxorubicin, or controls, which were vehicle-only, were added to samples. Analysis was with a Berthold illuminometer (see details in *Mirandola et al., 2011*) [72].

3.7 Chemotaxis assays.

U266 cells (400 x 103/well) were plated in 100-ml culture media with and without Gal-3C (0, 0.4, 2.0, 10, and 20 mg/ml) in 24-well transwell (8-μm pores) inserts. Media (600 ml) with B-cell chemoattractant stromal cell-derived factor (SDF)-1a (100 ng/ml; R&D Systems) was added to the bottom chamber. After 4 h, U266 cells in the bottom chamber were quantified on FACScan flow cytometer (2 min acquisition, 200 ms resolution) [72].

A similar procedure was used for HUVEC cells was preformed as reported in Leonardo et al., 2011 [72].

EGM-2 alone was used a negative control. Subsequent to 16-h incubation, cells were detached from the upper chamber, and migrated cells were pictured on the lower side of the filter after fixing and staining with 30% methanol + 10% acetic and 0.1% Coomassie Brilliant Blue.

Following several washing in filtered water, the transwell was air-dried. Pictures were taken with an inverted X71 microscope (Olympus America Inc., PA, USA).

3.8 Generating AAV/GFP genome and virus stocks.

The adeno-associated virus/green fluorescent protein (AAV/GFP) genome was designed as previously described in Mirandola et al., 2011 [72]. Virus stocks of AAV/GFP were generated using complementary plasmids in s96-0.8 plus a helper virus [72] using HEK293 cells. Subsequently, lysates of HEK293 cells as a mock and HEK293 cells infected. Following the generation of the virus stock and measuring the virus by real-time PCR [72], on an ABI [72, 102].

3.9 Testing Gal-3C and Bor in NOD/SCID mouse model of MM.

U266 cells were washed once in PBS (Sigma-Aldrich, St. Louis, MO, USA), counted, prior to injection [72]. U266 cells (1×10^7) were injected subcutaneously into the abdomen of naive NOD/SCID mice. The tumor masses were measured weekly with a pair of calipers. The formula: width 2x length x 0.5, where width is the smallest dimension [72] was used for tumor volume calculations.

Mice were divided in four groups (groups #1-4).

Group #1 Control group was inserted subcutaneously an implanted a 200-ml mini-osmotic pump with PBS.

Group #2 received Gal-3C (30 mg/d/mouse) of a total of 500 μg via a 200-ml mini-osmotic pump implanted abdominally over a 16-day period.

Group #3 received six doses of 15 mg Bor in 50-ul injections via the tail vein on days 1-2, 8-9, and 15-16 for a total of 90 mg.

Group #4 received Gal-3C (30 mg/d/mouse) via mini-pump for a total dose of 500 mg plus a total 90mg Bor in 21 days. Mice where sacrificed at day 35 by anesthesia and cervical dislocation, and a post-mortem examination were conducted on the whole animals and dissected organs [72].

3.10 Real-time PCR.

Total ribonucleic acid (RNA) was extracted from the U266 cells, and tissue cells from the tumors, spleen, kidney, stomach, heart, lung and liver by means of a Trizol-reagent (Sigma-Aldrich, St. Louis, MO, USA) and isolated with the Oligotex mRNA Mini Kit (QIAGEN, Valencia, CA, USA), after deoxyribonuclease enzyme (DNase) I digestion. First-strand complementary deoxyribonucleic acid (cDNA) synthesis was performed using oligo (dT) 15 primers. PCR primers were as follows: 5'-GCGTACTCTGATACTACAATGATG-3' and 5'-GGG GTTTTGGGTAAAGTCA-3' for AKAP4; and 5- CGGTCGCCACCATGGTGAGC-3' and 5'-GAGCCGTACCTGCTCGACATG-3' for GFP. The sizes of the primers were amplified for AKAP4 to 1100 base pairs (bp) and for GFP to 730 bp, respectively. The positive controls were the cDNA of the U266 cells, and the negative controls were the PCR reaction mixture with water in place of the cDNA. RNA integrity in each sample was checked by amplification of a β-actin gene segment [72].

3.11 Flow cytometric analysis.

FACs analyses were performed for AKAP-4, human IgE, IgG, (heavy chain) k, and λ light chains, as previously described [72]. Briefly, cells from liver, blood, U266, and tumor masses

were broken up into single cells suspensions in RT as described in Mirandola et al., 2011. Single cell suspensions were located into 250-ml flasks containing 3-ml of an enzyme solution that consisted of 0.14% collagenase type I (Sigma-Aldrich, St. Louis, MO, USA) and 0.01% DNase (2000 kU/mg of tissue; Sigma-Aldrich, St. Louis, MO, USA) in RPMI 1640. The tissues were filtered by a 150-mm pore-size nylon and washed twice in RPMI 1640 supplemented with 10% FBS and penicillin/streptomycin.

Cells were incubated with monoclonal antibodies raised against human Ig, AKAP-4 and NF-kB. or isotype matching antibodies (BD Biosciences, CA, USA) as negative controls [72]. Analysis was performed using a fluorescence-activated cell scanner (BD Biosciences).

3.12 ELISA for human AKAP-4, IgG, E, k, and λ light chain.

A direct ELISA was performed to measure the levels of human AKAP-4, IgG, IgE, k, and λ light chain levels as reported [51, 72]. Antibodies for immunoglobulins were purchased from BD Biosciences. The anti AKAP-4 antibody was from Santa Cruz Biotechnology. Signal intensity was measured on a Victor 2 multimodal microplate reader (PerkinElmer, MA, USA) at 450 nm. All samples were run in triplicates [72,73].

3.13 Tubule formation assay.

Tubule formation assay was used to measure angiogenesis *in vitro* and performed as described [52,72]. Briefly, growth factor–reduced Matrigel (Becton Dickinson, NJ, USA) was allowed to polymerize in the presence of 30 ng/mL recombinant basic fibroblastic growth factor (bFGF; R&D Systems MN, USA) for 1 h at 37°C (50 uL/well). HUVEC (5,000/well), serum-starved for 2 h prior to trypsinization, resuspended in 200 μL of serum-free EGM-2 supplemented with 20% V/V conditioned medium obtained after 48-h U266 treatment with 10 μg/mL Gal-3C, 5

nM BOR, 10 µg/mL Gal-3C + 5 nM BOR, or 0.6% V/V PBS (Gal-3C and BOR vehicle) as a control. The positive control was EGM-2 with 20 ng/mL VEGF (R&D Systems MN, USA), while the negative control was EGM-2 alone. Cells were seeded onto the polymerized Matrigel and incubated for 16 h at 37°C with 5% CO_2 to allow tubule formation. The assays were run in triplicate and pictures were taken with an inverted X71 microscope (Olympus America Inc., PA, USA) [72].

3.14 ELISA for VEGF and bFGF.

An ELISA was performed to measure the levels of VEGF and bFGF in media from U266 cells treated for 16 h with 10 µg/mL Gal-3C, 5 nM Bor, or 10 µg/mL Gal-3C with 5 nM Bor, or control media with PBS only. The levels of VEGF and bFGF were extrapolated using standard curves obtained by analysis of 10-fold serial dilutions (0-1,000 ng/mL) of purified recombinant proteins (Abcam, MA, USA).

Subsequently, plates were washed twice with PBS+0.025% V/V Tween-20 (300 µL/well) and incubated for 1 h at RT with anti-mouse or anti-rabbit HRP-labeled secondary antibodies (0.2 µg/mL in PBS, 50 µL/well Abcam, MA, USA). The plates were washed 3 times with PBS+0.025% V/V Tween-20 (300 µL/well), and then the TMB colorimetric substrate (Thermo Fisher Scientific, IL, USA) was added and absorbance was measured at 405 nm (0.1s) after 5 minutes on a Victor 2 multimodal microplate reader (PerkinElmer, MA, USA) at 450 nm. All samples were run in triplicates [72].

3.15 Statistical analysis.

All of the data was expressed as mean values ± 95% confidence interval. Results were analyzed using GraphPad Prism version 4.00 for Windows (GraphPad Software, San Diego, CA).

Univariate analysis was performed through a Student t test as required for parametric variables. A p value of less than 0.05 was considered statistically significant. Statistical analysis for tumor size was performed through one-way ANOVA test and a Tukey post-test was used to analyze the mean tumor volumes with a 95% confidence interval [72].

3.16 Immunohistochemistry.

The tissue array was baked following the company's instructions (DAKO, Carpinteria, CA, USA) at 60 ºC. After 15 minutes incubation in a 3% H_2O_2 solution, it was exposed at room temperature (RT) for 45 minutes to the anti-Akap-4 primary antibody (1:100 dilution in PBS/BSA 0.1%). After washing, sections were incubated for 30 minutes at RT with DAKO Envision system (DAKO, Carpinteria, CA, USA), followed by 5 minutes dark incubation with the DAB system (DAKO). Tissues were counter-stained with hematoxylin (Fisher Scientific, Pittsburg, PA, USA) and results were evaluated by light microscope (Leica DMLA, USA). Pictures were taken at 20X, 40X and 63X magnifications and analyzed by imaging software. [72, 73]

3.17 Immunocytochemistry and immunofluorescence.

MM plasma cells were spun in a cytospin column in the amount of $5x10^4$-10^5 cells per slide. After fixation with SlideRite (Fisher, USA) and overnight air drying, each sample was permeabilized (P) in a 0.1% Triton X-100 sodium citrate buffer, diluted in PBS, for 15 minutes at 4°C or left not permeabilized (NP). For immunocytochemistry, cells were exposed to the anti-Akap-4 primary antibody (1:100 dilution in PBS/BSA 0.1%), and then incubated for 30 minutes with the Envision System (DAKO) and 5 minutes with DAB (DAKO). The immunocytochemical reaction was observed using a light microscope. Pictures were taken at

40X and 100X objective magnifications and analyzed by imaging software. For immunofluorescence, cells were incubated overnight in a wet chamber at 4°C with anti-Akap-4 primary antibody (1:100 dilution in PBS/BSA 0.1%) and with PE conjugated rabbit IgG secondary antibody (1:500 dilution) (Abcam, USA). Results were analyzed by inverted fluorescence microscope (Olympus IX71 inverted microscope equipped with laser), pictures were taken at 20X and 40X objective magnifications, and analyzed by Flow-view software [72,73].

4. RESULTS

4.1 Galectin-3 expression in MM cell lines

Nine MM cells: MM-1S, MM-1RL, NCI-H929, RPMI-8226, 8226/Dox-40, 8226/LR-5, ARP-1, ARK-B, and U266 were evaluated by Western blot to identify galectin-3 protein.

Figure 4.1 shows that all of the cell lines have galectin-3 protein (~30 kDa). The levels of expression of galectin-3 in the nine MM cells are heterogenic; only U266 and NCI-H929 expressed the highest levels [72].

The M3/38 anti-galectin-3 antibody stained three other bands. Earlier studies indicate that this antibody binds the N-terminal domain of the full-length protein [48-55]. Galectin-3 is digested by mammalian metalloproteinases (MMPs) including MMP-2, -9, and -13 that primarily cleave the Ala62 –Tyr63 bond yielding a fragment of ~22 kDa containing the CRD and an N-terminal fragment [48-55]. The Gly32-Ala33 bond is an interchange site for cleavage by MMPs that yields a 27 kDa fragment including the CRD [53-54].

An additional band that comes out at approximately 75 kDa in size is of similar intensity in each sample. Galectin-3 can form non-covalent homodimers and higher order multimers by mediated binding of its N-terminal domain [55, 56]. Previous to electrophoresis, the samples were heated at 70 °C rather than boiled, thus, it is also possible that the 75 kDa bands were composed of non-covalent homodimers of galectin-3. Transglutamination should not be affected by reduction, but it is unlikely that disulfide bonds survived the treatment of the samples with the reducing agent, 2-mercaptoethanol [72].

FIGURE 4. 1

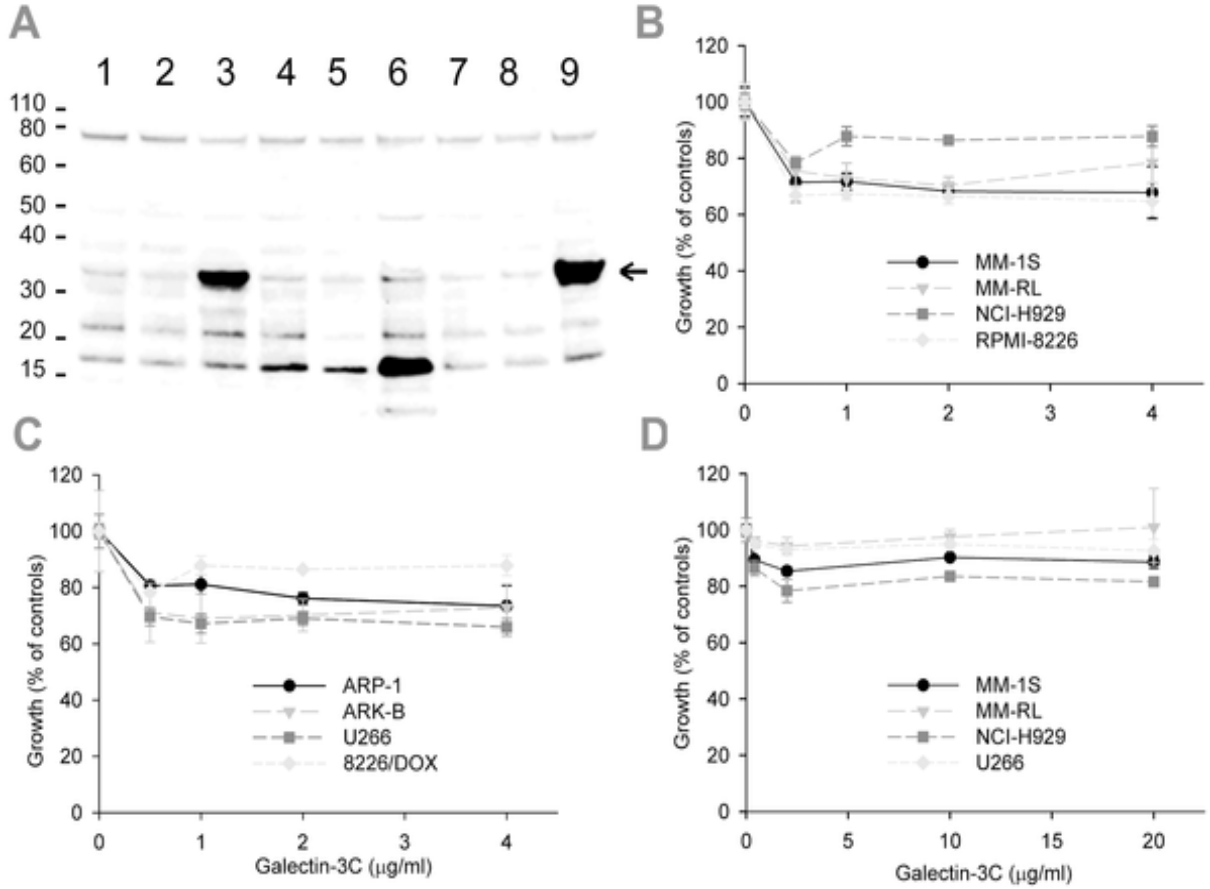

Figure 4.1. Galectin-3 expression levels in MM cell lines and effects of galectin-3 inhibition *in vitro.*

(**a**) The protein lysates of MM cells are: MM-1S; 2 MM-1RL; 3 NCI-H929; 4 RPMI-8226; 5 Dox-40; 6 LR-5; 7 ARP-1; 8 ARB-B; 9 U266. Protein fractions were analyzed by immunoblot to locate galectin-3 (30 kDa) (see arrow). (**b**) Shows the graph results from proliferation assays of MM-1S, MM-RL, NCI-H929, and RMPI-8266 and (**c**) ARP-1, ARK-B, U266, and 8226/Dox cells to 0.5, 1, 2, or 4 μg/ml Gal-3C compared to the control (48 h). Low proliferation when MM cell lines were treated with Gal-3C (defined as $P<0.05$; *t*-test) after 48 h. (**d**) Proliferation assays with MM-1S, MM-RL, NCI-H929, and U266 with different doses (0.4, 2, 10,or 20 μg/ml Gal-3C versus control wells over 24 h). Significant decrease ($P<0.01$) in proliferation of MM-1S, NCI-H929, and U266 cells in response to Gal-3C after 24 h. Error bars are ± S.D [72]

4.2 Gal-3C inhibits chemotaxis of U266 cells.

The adding together of Gal-3C to the media with U266 cells in the top chambers of bicameral transwell chambers (Figure 4.2) (P<0.001 for all Gal-3C treatments versus controls) decreased the migration of the cells into the bottom chamber containing SDF-1α, a potent lymphocyte chemotactic factor [56, 57, 60, 62, 64, 72]. The percentage of inhibition improved by more than 70% using 2.0 μg/ml Gal-3C in contrast to a 0.4 μg/ml. Nevertheless, mounting the concentration to 10 and 20 μg/ml generated only a little higher percentage of inhibition in contrast to 2.0 μg/ml [72].

FIGURE 4.2

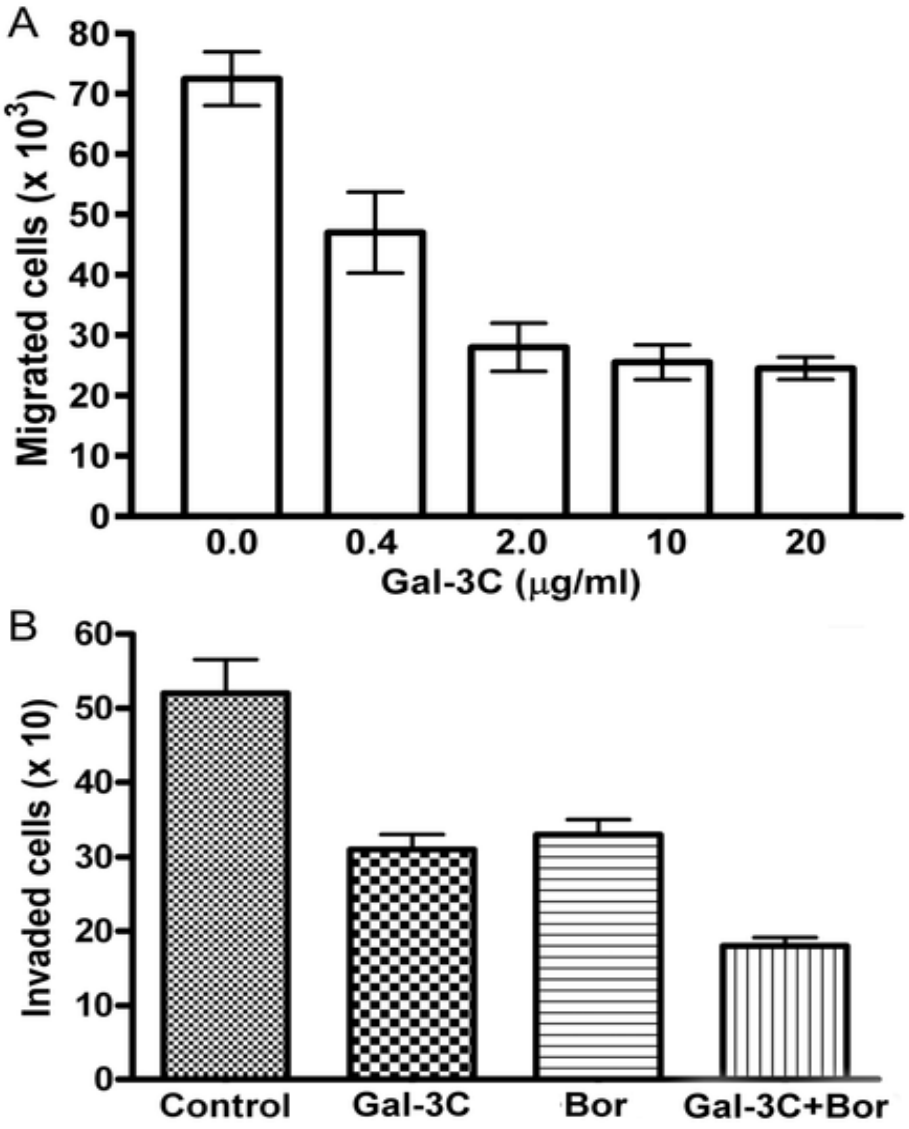

Figure 4.2. Gal-3C inhibits the chemotaxis and invasion of U266 MM cells.

(**a**) Chemotaxis of U266 was significantly reduced by Gal-3C (0.4, 2, 10, or 20 μg/ml) in response to SDF-1α (100 ng/ml). Error bars are ± S.D. and sextuplicate data points are represented (ANOVA with Tukey test $P<0.001$ for all, compared to controls).
(**b**) Significant reduction in the invasion activity of U266 by Gal-3C and Bor. Experiments were repeated three times. Error bars represent ±SD [72].

4.3 Generation and testing of AAV/GFP virus stocks

A map of the AAV/GFP vector is shown in Figure 4.3. XbaI and NotI were used as a restriction sites to insert the GFP gene downstream of the p5 promoter. Figure 4.3B illustrates the identification of AAV/GFP by restriction enzyme analysis. XbaI and NotI enzymes cut GFP from AAV/GFP. The titers of virus stocks were determined by real-time PCR (Figure 4.3B) to be 10^8 encapsulated genomes (eg). Subsequent to the generation of the AAV/GFP virus stock, the infection of U266 cells was analyzed. U266 cells were infected with AAV/GFP, and confirmed the infection by immunofluorescence labeling, RT-PCR, and cytofluorimetric analysis (Figs. 4.3C and 4.3D) [72,102].

FIGURE 4. 3

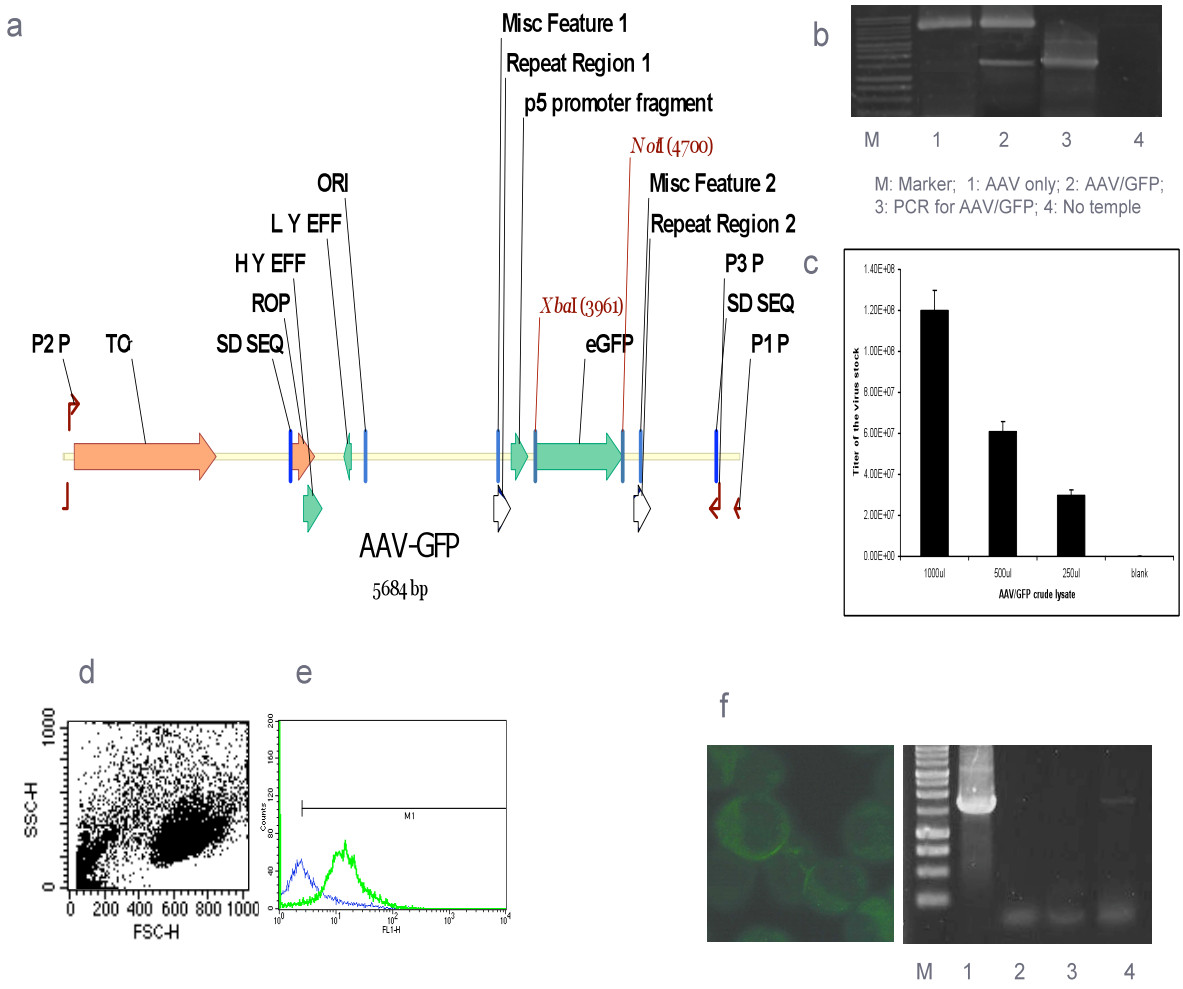

Figure 4.3. Viral vectors and analysis of infection.

(A) A map of the AAV/GFP. Xba I and Not I were used as restriction enzymes to insert the GFP coding sequence. (B) The ligation of AAV genome and GFP. The GFP insert was extracted from AAV/GFP by Xba I and not I (lane 2). (C) Quantification of virus titers by real-time PCR. (D) Identification of U266 cells transduced with AAV/GFP by flow cytometry. (E) RT-PCR for GFP expression in transduced U266 cells. M: Marker, 1: AAV/GFP plasmid, 2: No RT 3: No template, 4: U266 cells transfected with AAV/GFP. (F) Photo of U266 cells showing fluorescence of AAV/GFP-transduced U266 cells [72].

4.4 Gal-3C and Bor synergistically inhibited endothelial cell migration

Chemotaxis assays were performed to assess the effects of Gal-3C on MM cell-induced migration of endothelial cells, using a Transwell®-based platform. U266 cells were cultured in media in the presence of 10 μg/mL Gal-3C, 5 nM Bor, the combined treatment, or control (PBS)-only, following 48 h of conditioned media (c.m.) produced by U266 cells. The U266 were used in different treatments with 20% diluted EBM-2 medium and human umbilical cord vascular endothelial (HUVEC) cells. Results of a 16-h migration assay are shown in Figure 4.4a and 4.4b. [68,72]. Matrigel™-based tubule formation assay was performed to assess the effects of diverse treatments on the ability of U266 cells to stimulate angiogenesis [68-72, 87]. Results show that treatment with Gal-3C or Bor only, and in combination, almost completely blocked the potential of U266 cells for induction of angiogenesis (Figure 4.4.c) [72, 74].

FIGURE 4.4

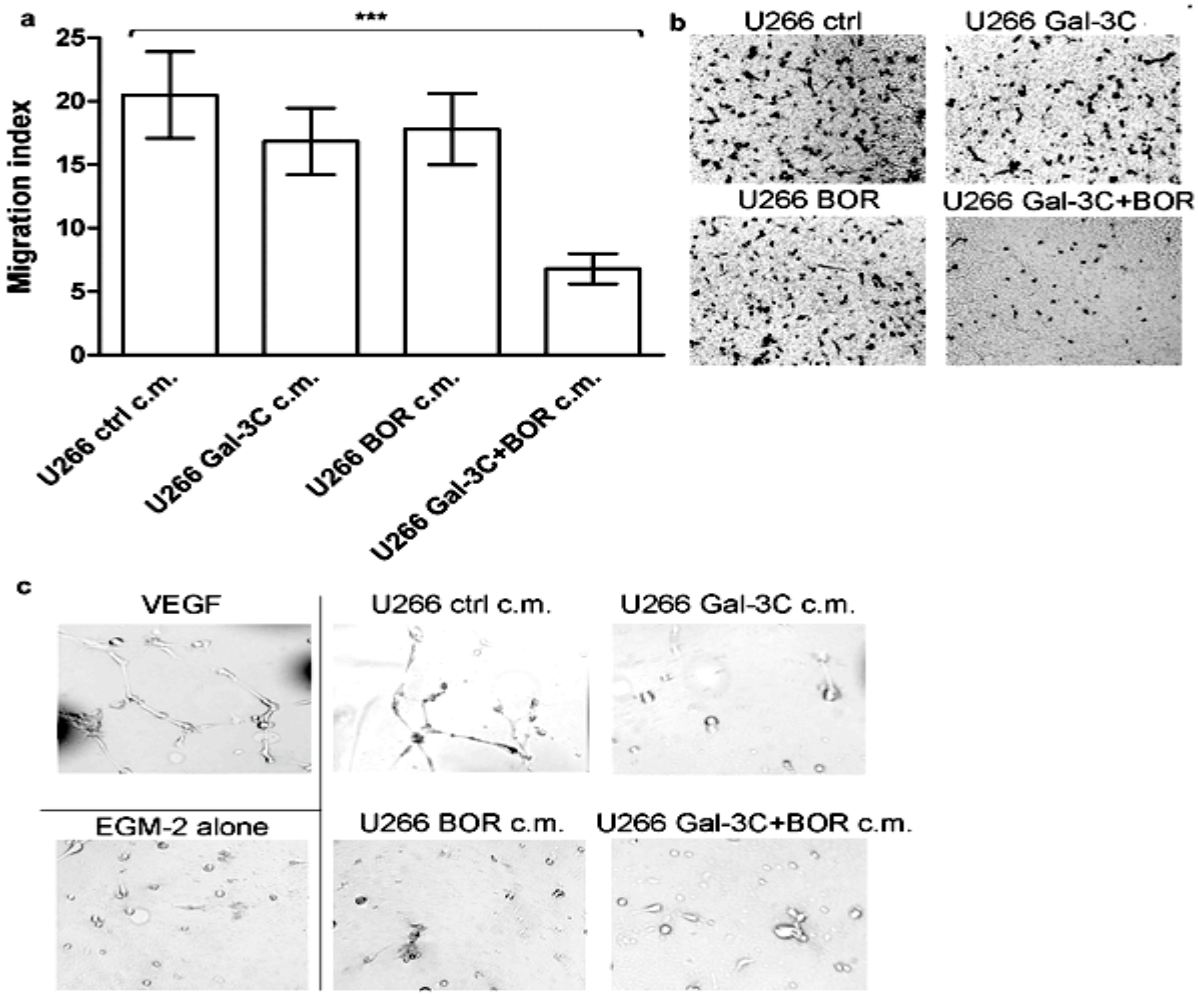

Figure 4.4 Vascular endothelial cell migration and tubule formation.

(**a**) Migration index graph [72]. Mean migration indices (error bars are ± SD) were expressed as the number of cells migrated in the presence of the indicated stimuli divided by the number of cells migrated in the presence of EBM-2 alone [72]. (**b**) Representative pictures of the filters. (**c**) Representative pictures of tubule formation with different conditions [72].

4.5 Gal-3C did not affect endothelial cell viability.

To establish if the effects of Gal-3C alone or in combination with Bor on vascular endothelial cell migration or secretion were due to reduced cell viability, the HUVEC cells were treated with Gal-3C, Bor, or both agents for 48 h. The viability for U266 was measured. Since at the highest concentrations, Gal-3C had a low effect on HUVEC viability and Bor alone showed an impressive inhibition, Gal-3C (2 μg/ml) and Bor (1 nM) were used for the chemotaxis assays. Results were run in triplicate, see figure 4.5 [72].

FIGURE 4.5

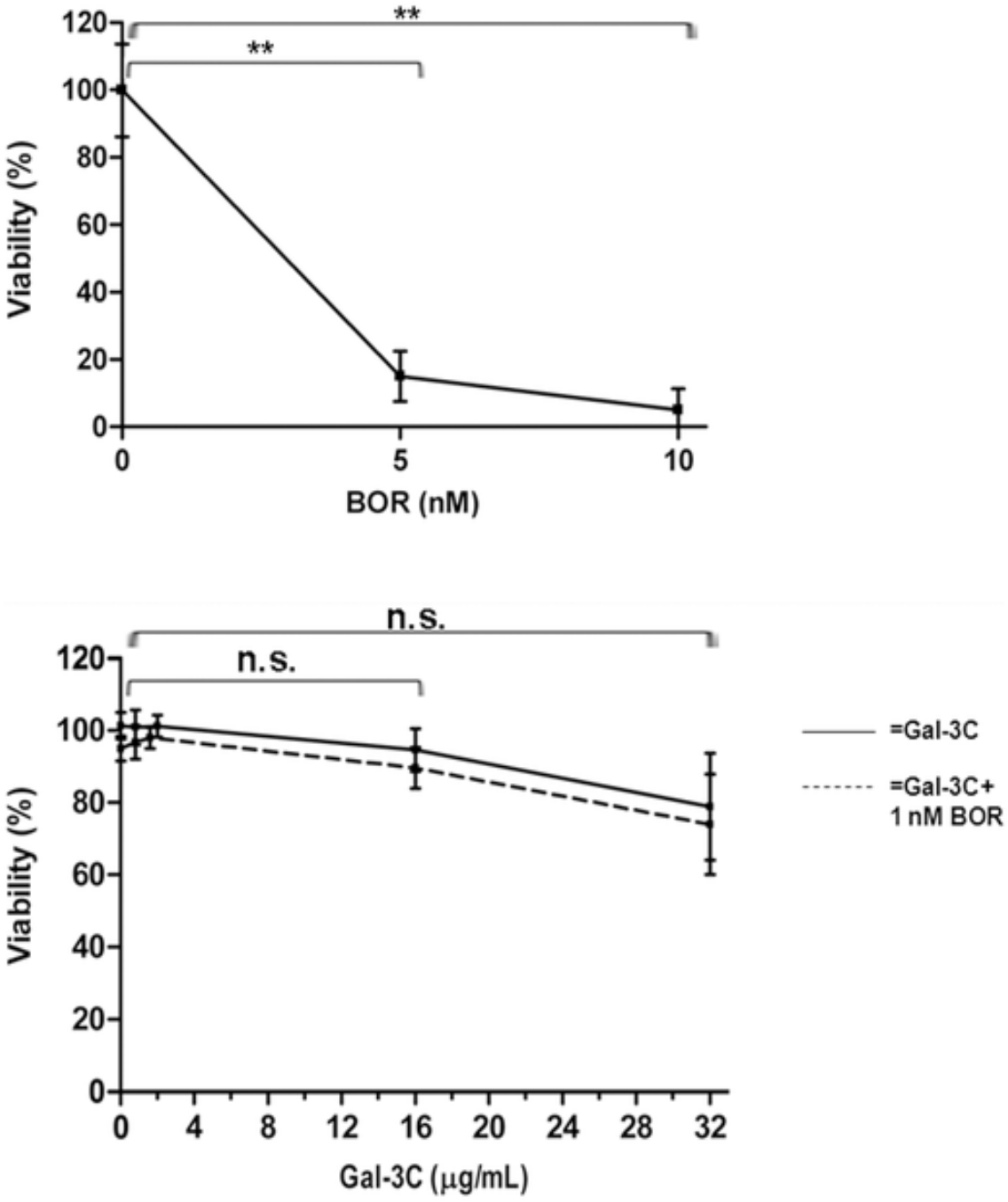

Figure 4.5. Vascular endothelial cell viability assay.

Representative of viability of a U266 cells assay. Experiments were run in triplicate and displayed as percentage of control (untreated) cells. The graphs show mean values and error bars represent ± SD. **ANOVA Tukey's post test $P<0.01$. n.s. = not significant [72].

4.6 Gal-3C and Bor reduced αvβ3 integrin clustering in HUVEC cells

To assess the effects of the ability of U266 cells to provoke integrin engagement on endothelial cells, HUVEC cells were incubated with c.m. produced by U266 cells cultured in 10 μg/mL Gal-3C, 5 nM Bor, or the combination for 48 h. Pictures were taken by a confocal (see Figure 4.6). Figure 4.6 show that Gal-3C and Bor, in combination, blocked the development of clusters of αvβ3 integrins. Cluster of αvβ3 integrins were detected only in control wells. [72, 93-97,100, 101].

FIGURE 4.6

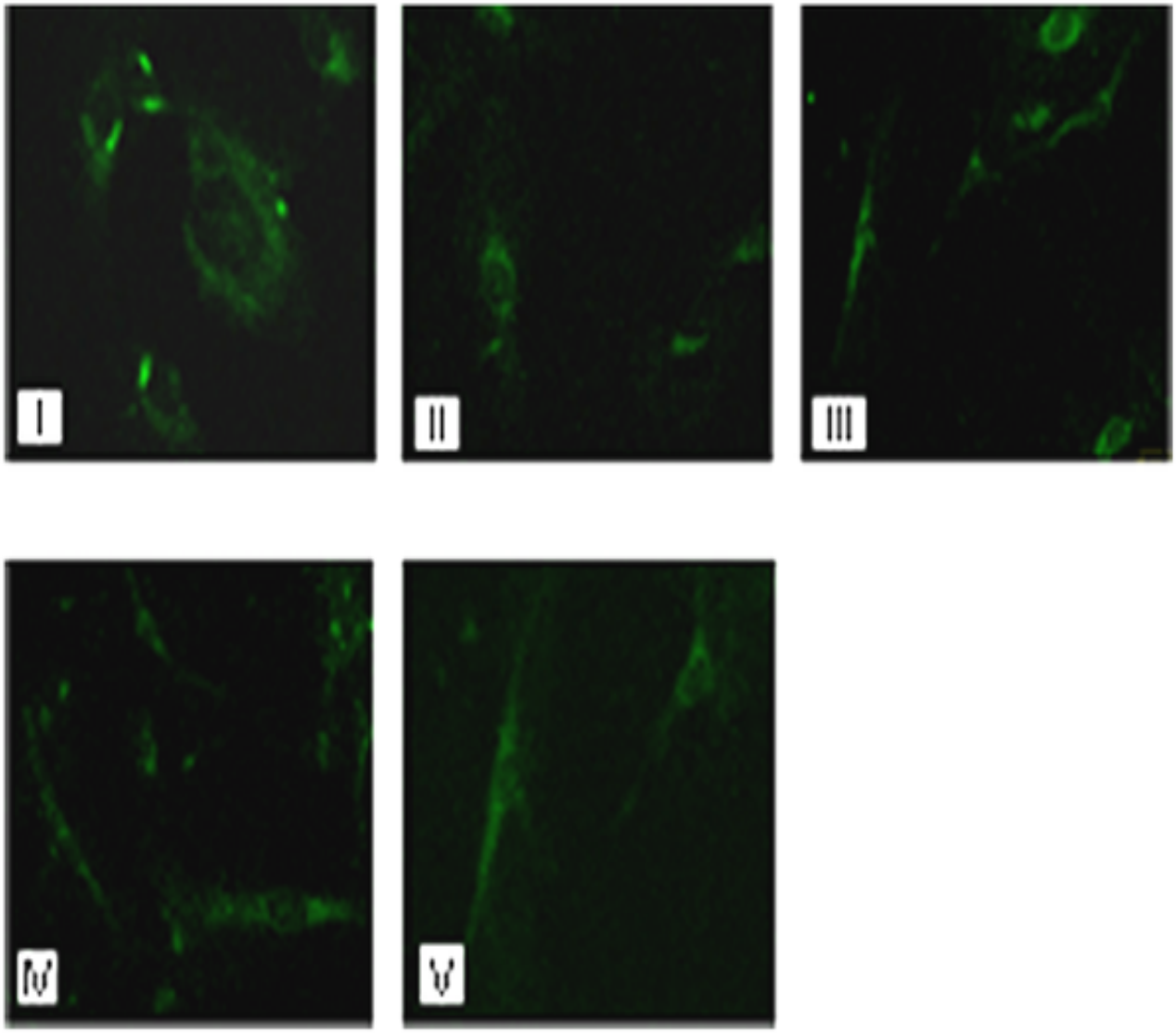

Figure 4.6. αvβ3 integrin clustering assay.

Representative pictures of HUVEC cells were fixed and stained with anti-αvβ3 antibody. Integrin clusters are evidenced as high-density spots in the HUVEC treated with U266 c.m. (I). HUVEC cells treated with different conditions showed less integrin cluster represented by the expression of spots as Gal-3C (II) Bor (III) or Gal-3C+Bor (IV). HUVEC cells treated with EGM-2 medium alone showed no clusters (V). The figure shows representative photomicrographs obtained by confocal microscopy (60X magnification) from three independent experiments [72].

4.7 Gal-3C and Bor inhibited secretion of VEGF and bFGF by U266 MM cells.

ELISA was carried out to determine the levels of VEGF and bFGF in media from U266 cells treated with 10 μg/mL Gal-3C, 5 nM Bor, Gal-3C with Bor, or control media with vehicle (PBS) only, for 16 h (Figure 4.7) [72, 87].

FIGURE 4.7

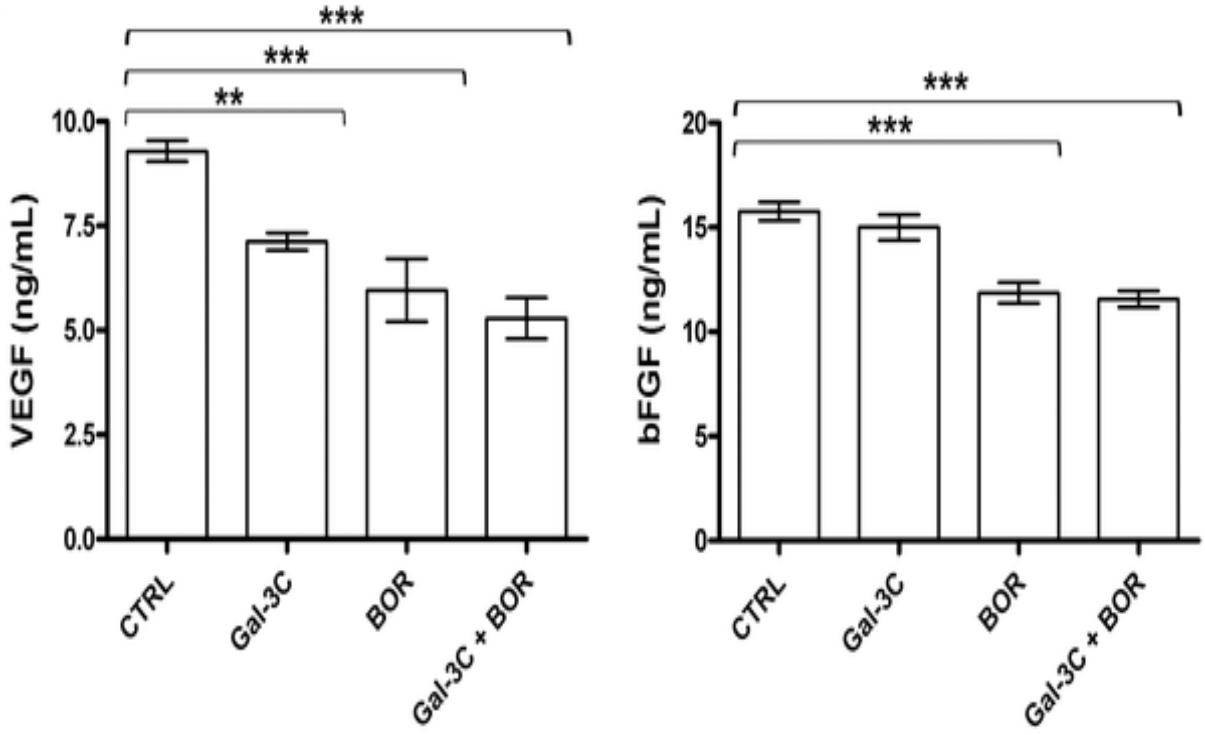

Figure 4.7. Molecular effects of Gal-3C and Bor on U266 cells.
Representative ELISA after 48 h for the measurement of VEGF and bFGF is shown. Histograms represent mean values of 3 independent experiments. Error bars indicate ± SD. Statistical analysis was performed through one-way ANOVA and Tukey's post-test: **P<0.01; ***P<0.001 [72].

4.8 Growth of U266 tumors was inhibited by Gal-3C alone, and Gal-3C with Bor

To determine the U266 MM model in the NOD/SCID mice, the treated mice were injected with Gal-3C, Bor, and combination of Gal-3C and Bor (Figure 4.8a). In figure 4.8b, the tumor volume was measured with calipers once weekly is shown.

In the group of mice treated with Bor, the tumor volume was less than in the untreated group from d 28 through d 35 (unpaired t test $P<0.001$), whereas the group of mice treated with Gal-3C and Bor+Gal-3C showed smaller tumor masses than the control group (82% and 61%, respectively) (unpaired t test $P<0.001$).

The groups receiving the combination of Gal-3C with Bor had less tumor mass of the groups treated with Bor (or with Gal-3C) starting on d 21 (unpaired t test $P<0.001$).

The mice that were treated with Gal-3C generated fewer and smaller tumor masses versus the mice treated with Bor, starting on d 21 (unpaired t test $P<0.001$), with a mean difference between the two of 4.431±1.494 mm3, through d 35 when the mean difference was 31.54±4.379 mm3 (unpaired t test $P<0.001$).

The combination therapy had the greatest effect at day 35, with a reduction of 94% in the mean tumor volume, versus the untreated group (unpaired t test $P<0.001$) [72].

FIGURE 4.8

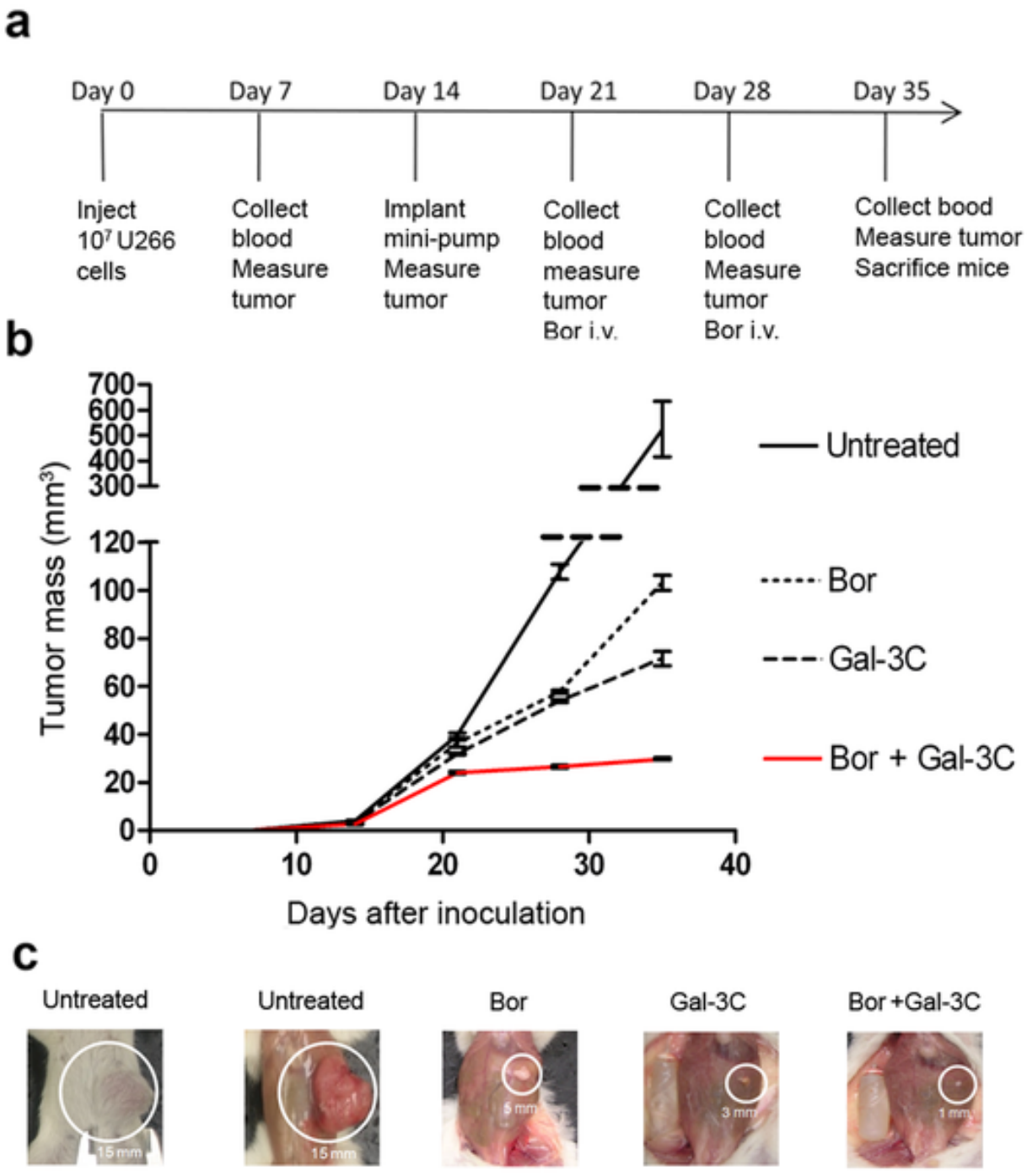

Figure 4.8. Experimental design and outcome of Gal-3C treatment in NOD/SCID MM xenografts.

(**a**) Schedule of tumor challenge, drug administration, and sample collections. (**b**) Graph of tumor masses showing Gal-3C with different treatments (untreated, Bor, Gal-3C and Bor plus Gal 3-C) [72].

4.9 Analyses of AKAP-4 and GFP expression.

To analyze the mRNA of the AKAP-4 and GFP by RT-PCR, specimens of the subcutaneous tumors (see Figure 4.9) were collected. These results showed the mRNA expression of both GFP and AKAP-4 and established that the tumor masses originated from U266 cells (Figure 4.9) [72].

FIGURE 4.9

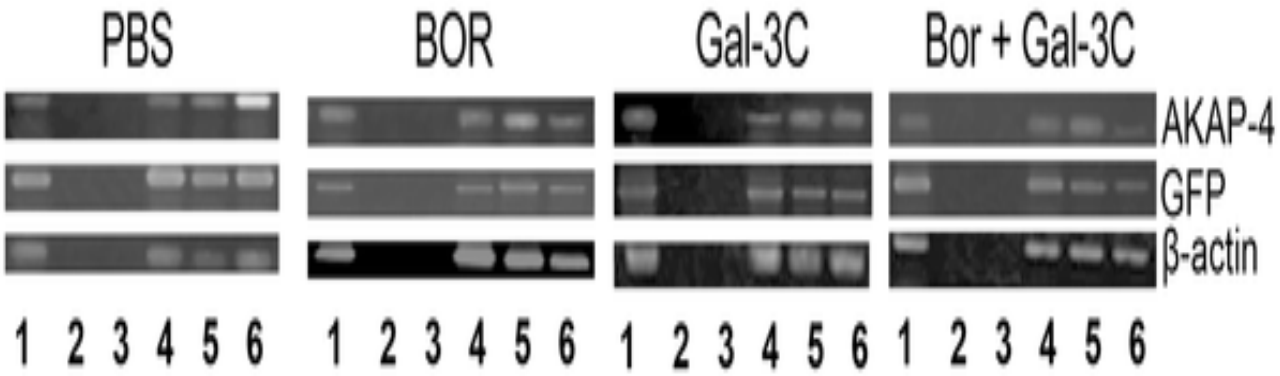

Figure 4.9. Analysis of AKAP-4 and GFP expression.

Depiction of RT-PCR showed the expression of AKAP-4 and GFP in different treatments (PBS, Bor, Gal-3C, and Bor plus Gal-3C) [72].

4. 10 ELISA for human immunoglobulins and AKAP-4 in mouse serum.

AKAP-4 also was identified in the sera of tumor-bearing mice (Figure 4.10 bottom panel). The increased AKAP-4 levels were associated with tumor growth. The serum starting in the vehicle-only group on d 21 was analyzed. At 35 d after injection the level of AKAP-4 in the sera from the combination therapy (Gal-3C plus Bor) group was less than the control group [72].

FIGURE 4.10

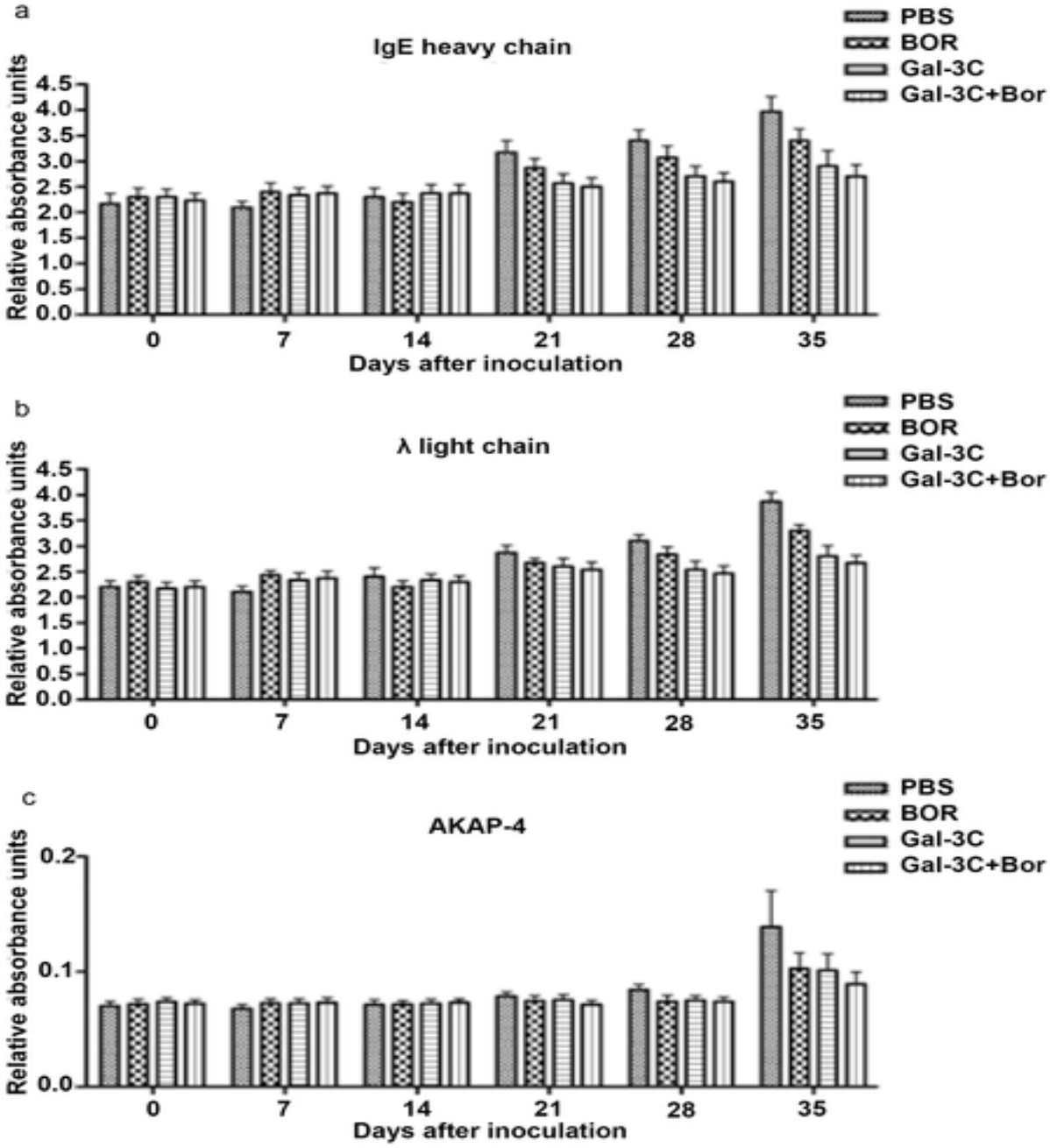

Figure 4.10. ELISA for human immunoglobulins and AKAP-4 in mouse serum.

ELISA measured the levels of immunoglobulins and AKAP-4. Each graph is representative of three experiments with samples analyzed in triplicates, and the error bars represent ± SD [72].

4.11 Flow cytometric analyses of the expression of IgE and IgG.

FACs established the expression of IgE and Igλ by the tumors (Figure 4.11). The expression of IgE, Igλ and AKAP-4 were higher in the tumors of the control group. These results are similar to the results to the previous analysis [72].

FIGURE 4.11

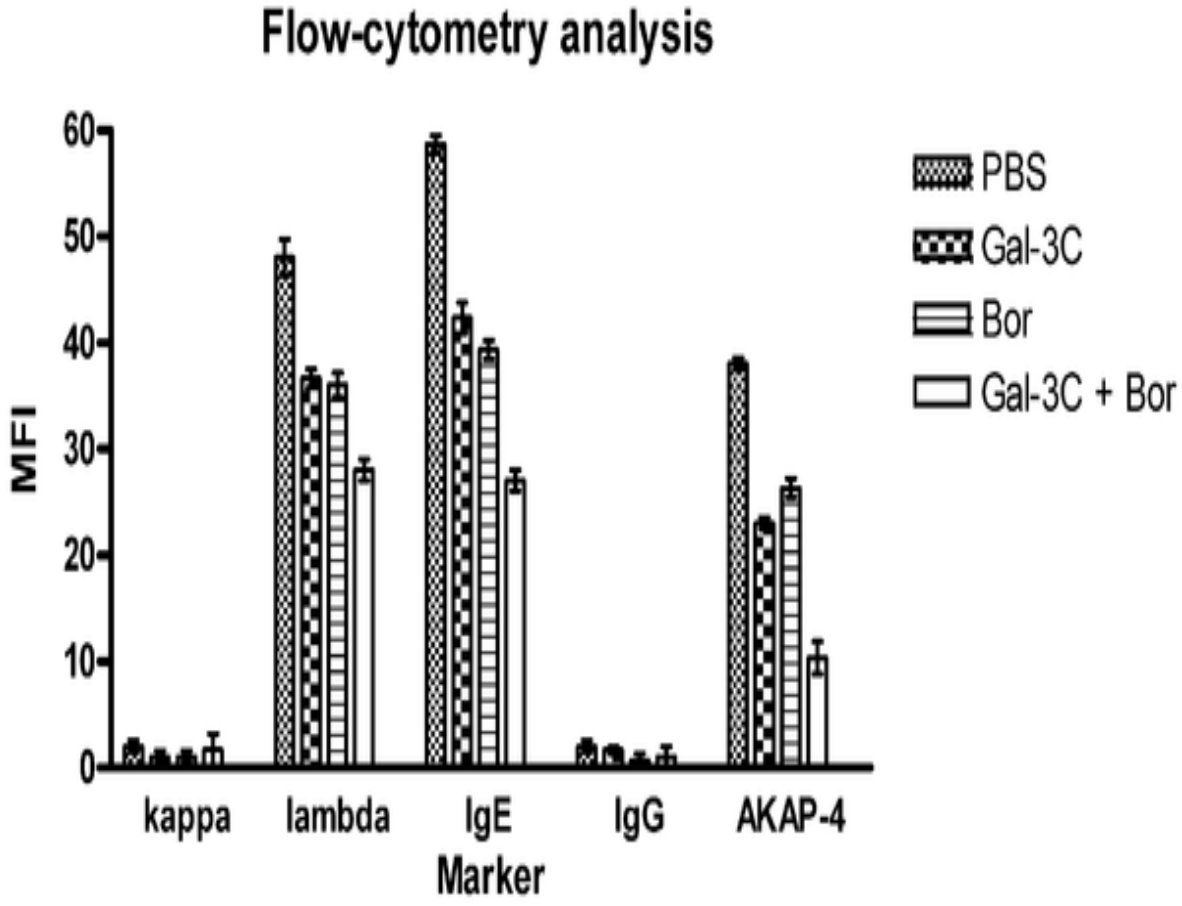

Figure 4.11. Flow cytometric analyses of the expression of IgE, IgG, Igκ, Igλ, and AKAP-4.

FACs analyses of the expression of immunoglobulins and AKAP-4. Single cell suspensions were obtained from liver, blood and tumor masses of different groups of mice treated with different conditions (PBS, Gal-3C, Bor, and Bor plus Gal-3C) [72].

4. 12 Molecular effects of Gal-3C and BOR on U266 cells.

After 48 h in the presence of indicated treatments, the levels of active NF-kB (serine 529 phosphorylated p65 subunit) were evaluated in U266 cells by flow-cytometry. Left, dot-plot; right, distribution of fluorescence intensity (filled gray histogram: control; bold black line: Gal-3C alone; gray line: BOR alone; thin black line: Gal-3C + BOR). **c)** Possible mechanisms of Gal-3C and BOR interaction in MM cells (see figure 4.12). Inactive NF-kB is located in the cytoplasm where it forms complexes with IKBα. Upon IKK-mediated phosphorylation, IKBα dissociates from NF-kB complex (p50 and p65 proteins). Free NF-kB is then phosphorylated on serine 529 of the p65 subunit and finally enters the nucleus where it regulates the transcription of target genes. It is known that administration of BOR administration to MM cells in culture activates the canonical NF-kB pathway by the inhibitor of nuclear factor kappa-kinase IKKβ phosphorylation, while galectin-3 promotes the activation of IKKα, also resulting in induction of NF-kB pathway.

Therefore, the contemporary administration of IKK inhibitors or Gal-3C with BOR is expected to have synergistic effects on MM cytotoxicity [76-85, 100].

FIGURE 4.12

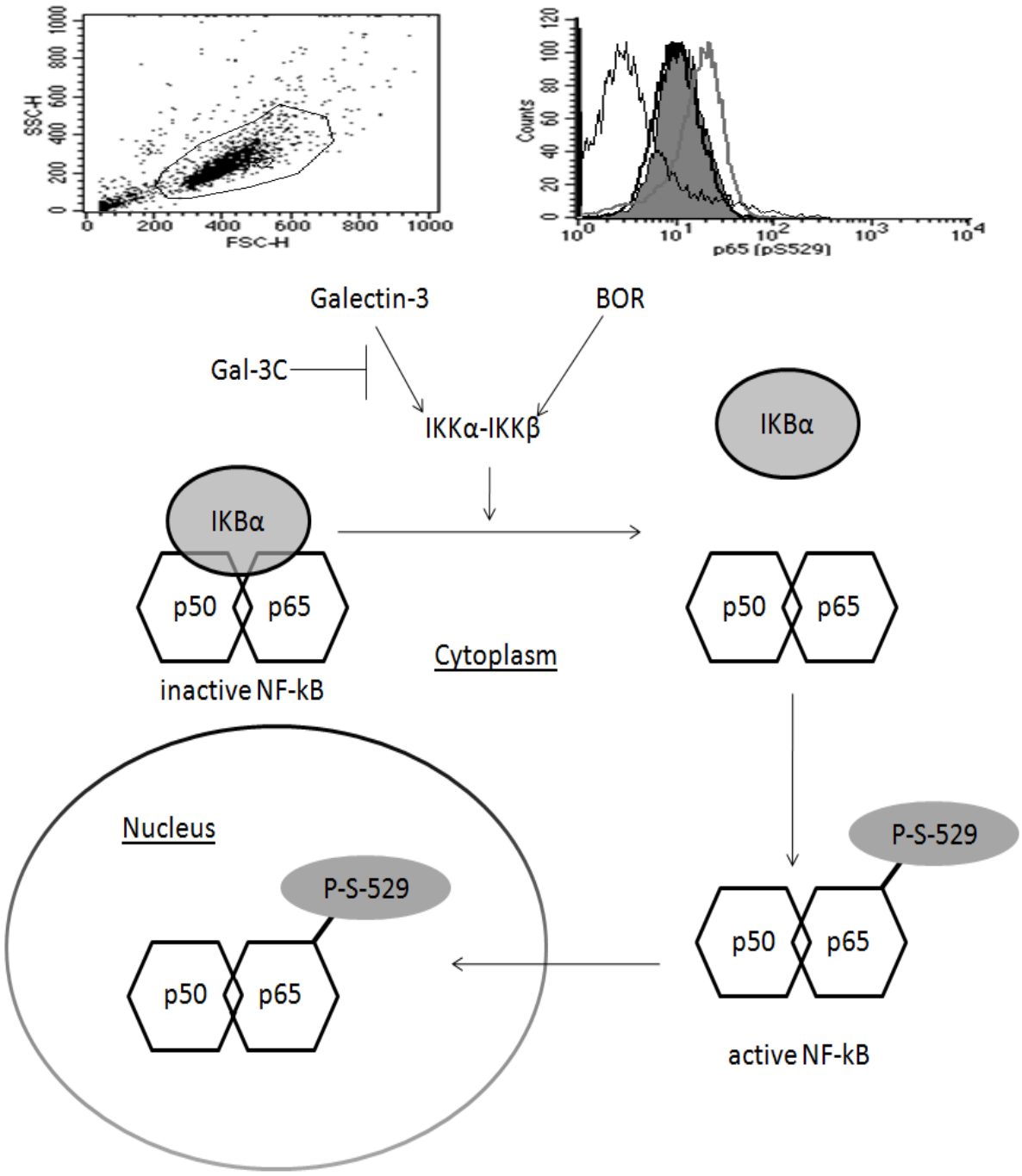

Figure 4.12. Molecular effects of Gal-3C and BOR on U266 cells.

5. Discussion

The standard treatment for MM is based on high-dose chemotherapy, radiotherapy, and autologous hematopoietic stem cell transplantation. MM is still not well-understood and remains a fatal hematological disease.

Bor was approved by the FDA in 2003 to treat refractory MM by the FDA [4, 18, 23, 45, 46, 50, 81, 82]. Remarkably, Bor alone or in combination with thalidomide or lenalidomide, offers up to 85% response rates, but more 95% of the patients ultimately relapse [45,46, 50, 56,57].

In this study, Gal-3C, in single or in combination with Bor, was evaluated *in vivo* using a NOD/SCID mouse model using human MM cells.

Furthermore the *in vitro* analysis was not as effective and showed that Gal-3C has a low inhibition to the proliferation of all 8 MM cell lines (see Figure 4.1). I hypothesized that the low effect *in vitro* was due to inhibition of galectin-3 [57, 58, 59]. Nevertheless, Gal-3C alone or in combination is more effective *in vivo*. The results show that Gal-3C has anti angiogenesis effects in MM.

Moreover angiogenesis plays a major role between MM cells and the tumor environment [68-70]. VEGF has been described in the literature [71-74] that is the main mediator of MM-induced angiogenesis [71-74].

Galectin-3 has been described by Li WW, et al. to inhibit VEGF-mediated angiogenesis [74].I hypothesize that the effects of Gal-3C *in vivo* inhibits the angiogenesis process produced by the engrafted U266 cells. The results show that the combination of Gal-3C and Bor creates significantly less HUVEC migration and angiogenesis (Figures 4.3, 4.4) [72]. The single treatments inhibited the angiogenesis process but not the migration. Integrins such as $\alpha v\beta 3$ are important in the process of angiogenesis [72].

In Figure 4.5, the collective use of Bor and Gal-3C and the single treatment can block αvβ3 integrin activation [72].

The ELISA assays showed that single and/or combination (Gal-3C and Bor) diminished the ability for the U266 to secrete VEGF. Only when Bor was used alone there was a decline in bFGF levels (Figure 4.6). These results indicate that Gal-3C and/or Bor obstruct HUVEC migration and *in vitro* angiogenesis by the down-regulation of VEGF and bFGF [72].

The Gal-3C is shown to be more effective in the *in vivo* model due to the interactions with tumor environment. [60-63,72]. Gal-3C inhibited tumor growth in a NOD/SCID mouse model of MM to a greater extent than Bor. Combining Gal-3C with Bor caused greater reduction than either alone, promising proof-of-concept data that justifies proceeding towards human clinical testing.

Bor is one of the most effective drugs for MM, and is incorporated into front-line care. Bor is beneficial in combination therapies [85], but often becomes ineffective due to resistance and display of off-target toxicity [87]. New combination therapies with Bor may facilitate better patient outcomes.

The *in vivo* activity of Gal-3C in the U266 s.c. NOD/SCID model was largely mediated by interactions involving the tumor microenvironment [86] through angiogenesis and inhibition of adhesion [87]. The data are supported by recent results of Markowska *et al*. who showed that Gal-3C inhibited VEGF-mediated angiogenesis, and that galectin-3 induces angiogenesis [88]. Inhibition of U266 cell chemotaxis in response to SDF-1α also demonstrated the potential anticancer activity of Gal-3C in human MM. Galectin-3 has been shown to bind to mucin-1 [87-88], a glycosylated oncoprotein, which is important in tumorigenicity and metastasis of cancers [87, 89] including MM [90-93], β1integrins [94-97] that modulate MM adherence to fibronectin stimulating transcription of proto-oncogenes [98-100], and SDF-1α [101]. The tumor marker,

cancer testis antigen (CTA), AKAP-4 (highly expressed in MM cells) [11, 73] was used. The ELISA showed that heavy and light chain IgE and AKAP-4 levels were less in treated groups versus to the control group on d 21, 28, and 35 (Figure 4.10).

These results were repeated by a FACs analysis of IgE and Igλ on cells from MM tumors (Figure 4.10), confirming the previous data [72,73]. AKAP-4 was previously studied as a tumor marker for MM [47].

The expression of AKAP-4 and GFP was low in the treated group with Gal-3C and Bor, confirming the results with IgE and Igλ [72,73].

In MM cells specifically, Bor has been shown to induce the canonical NF-κB pathway by triggering IKKβ-mediated phosphorylation of IKBα [74-75, 77]. Earlier studies show that galectin-3 can stimulate the NF-κB path downstream targeted genes, and that inhibition of galectin-3 with modified citrus pectin (GCS-100) [66-76] damages TNF-α provoked initiation of NF-κB by obstructing IKKα phosphorylation of MM cells [66, 67-72],

5. 1 Conclusion

In conclusion, the overall goal of this research is the development of a novel human protein, Gal-3C, as a treatment for multiple myeloma (MM) that can be administered with other agents to facilitate the induction of apoptosis, and anti-angiogenesis effects and to increase the percentage of patients who are responsive to therapy, and their survival rate. MM is rarely curable despite the introduction of new therapeutic regimens, and more efficacious treatments are needed.

The results present proof-of-principle for the further study of the activity of Gal-3C in MM and justify the initiation of a Phase I clinical trial.

5.2 References

1. Bergsagel DE. (1991) Plasma cell myeloma: biology and treatment. Annu Rev Med; 42: 167-178.

2. Balakumaran A, Robey PG, Fedarko N, Landgren O. (2010) Bone marrow microenvironment in myelomagenesis: its potential role in early diagnosis. Expert Rev Mol Diagn; 10: 465-480.

3. Kuehl WM, Bergsagel PL. (2002) Multiple myeloma: evolving genetic events and host interactions. Nat Rev Cancer; 2: 175-187.

4. Bataille R, Harousseau JL. (1997) Multiple myeloma. N Engl J Med; 336: 1657-1664.

5. Greipp PR, San Miguel J, Durie BG, Crowley JJ, Barlogie B, Blade J, Boccadoro M, Child JA, Avet-Loiseau H, Kyle RA, Lahuerta JJ, Ludwig H, Morgan G, Powles R, Shimizu K, Shustik C, Sonneveld P, Tosi P, Turesson I, Westin J. (2005) International staging system for multiple myeloma. J Clin Oncol; 23: 3412-3420.

6. Koomen JM, Haura EB, Bepler G, Sutphen R, Remily-Wood ER, Benson K, Hussein M, Hazlehurst LA, Yeatman TJ, Hildreth LT, Sellers TA, Jacobsen PB, Fenstermacher DA, Dalton WS. (2008) Proteomic contributions to personalized cancer care. Mol Cell Proteomics; 7: 1780-1794.

7. Zhan F, Huang Y, Colla S, Stewart JP, Hanamura I, Gupta S, Epstein J, Yaccoby S, Sawyer J, Burington B, Anaissie E, Hollmig K, Pineda-Roman M, Tricot G, van Rhee F, Walker R, Zangari M, Crowley J, Barlogie B, Shaughnessy JD, Jr. (2006) The molecular classification of multiple myeloma. Blood; 108: 2020-2028.

8. Chiriva-Internati M, Ferrari R, Yu Y, Hamrick C, Gagliano N, Grizzi F, Frezza E, Jenkins MR, Hardwick F, D'Cunha N, Kast WM, Cobos E. (2008) AKAP-4: a novel cancer testis antigen for multiple myeloma. Br J Haematol; 140: 465-468.

9. Yeung J, Chang H. (2008) Genomic aberrations and immunohistochemical markers as prognostic indicators in multiple myeloma. J Clin Pathol; 61: 832-836.

10. Paiva B, Vidriales MB, Cervero J, Mateo G, Perez JJ, Montalban MA, Sureda A, Montejano L, Gutierrez NC, Garcia de Coca A, de Las Heras N, Mateos MV, Lopez-Berges MC, Garcia-Boyero R, Galende J, Hernandez J, Palomera L, Carrera D, Martinez R, de la Rubia J, Martin A, Blade J, Lahuerta JJ, Orfao A, San Miguel JF, Groups GPCS. (2008) Multiparameter flow cytometric remission is the most relevant prognostic factor for multiple myeloma patients who undergo autologous stem cell transplantation. Blood; 112: 4017-4023.

11. Atanackovic D, Hildebrandt Y, Jadczak A, Cao Y, Luetkens T, Meyer S, Kobold S, Bartels K, Pabst C, Lajmi N, Gordic M, Stahl T, Zander AR, Bokemeyer C, Kroger N. (2009) Cancer-testis antigens MAGE-C1/CT7 and MAGE-A3 promote the survival of multiple myeloma cells. Haematologica; 95: 785-793.

12. Atanackovic D, Luetkens T, Hildebrandt Y, Arfsten J, Bartels K, Horn C, Stahl T, Cao Y, Zander AR, Bokemeyer C, Kroger N. (2009) Longitudinal analysis and prognostic effect of cancer-testis antigen expression in multiple myeloma. Clin Cancer Res; 15: 1343-1352.

13 Nadav-Dagan L, Shay T, Dezorella N, Naparstek E, Domany E, Katz BZ, Geiger B. Adhesive interactions regulate transcriptional diversity in malignant B cells. (2010) Mol Cancer Res; 8: 482-493.

14. Cao Y, Luetkens T, Kobold S, Hildebrandt Y, Gordic M, Lajmi N, Meyer S, Bartels K, Zander AR, Bokemeyer C, Kroger N, Atanackovic D. (2010) The cytokine/chemokine pattern in the bone marrow environment of multiple myeloma patients. Exp Hematol 38 (10): 860-7.

15. Engelhardt M, Kleber M, Udi J, Wasch R, Spencer A, Patriarca F, Knop S, Bruno B, Gramatzki M, Morabito F, Kropff M, Neri A, Sezer O, Hajek R, Bunjes D, Boccadoro M, Straka C, Cavo M, Polliack A, Einsele H, Palumbo A. (2010) Consensus statement from European experts on the diagnosis, management, and treatment of multiple myeloma: from standard therapy to novel approaches. Leuk Lymphoma; 51: 1424-1443.

16. Azais I, Brault R, Debiais F. (2010) New treatments for myeloma. Joint Bone Spine; 77: 20-26.

17. Blade J, Carreras E, Rozman C, Sierra J, Rovira M, Batlle M, Valls A, Algara M, Marin P, Urbano-Ispizua A, et al. (1995) [Allogenic bone marrow transplantation in multiple myeloma. Analysis of 12 consecutive cases]. Med Clin (Barc); 105: 1-4.

18. Engelhardt M, Kleber M, Udi J, et al. (2010) Consensus statement from European experts on the diagnosis, management, and treatment of multiple myeloma: from standard therapy to novel approaches. Leuk Lymphoma; 51: 1424-1443. Review.

19. Ahmann GJ, Chng WJ, Henderson KJ, et al.(2008) Effect of tissue shipping on plasma cell isolation, viability, and RNA integrity in the context of a centralized good laboratory practice-certified tissue banking facility. Cancer Epidemiol Biomarkers Prev; 17:666-673.

20. Richardson PG, Sonneveld P, Schuster MW, et al. (2002) Bortezomib or high-dose dexamethasone for relapsed multiple myeloma. N Engl J Med; 2005; 352: 2487-2498.

21. Adams J. (2004) The proteasome: a suitable antineoplastic target. Nat Rev Cancer; 4:349-360.

22. Anderson KC. (2007) Targeted therapy of multiple myeloma based upon tumor-microenvironmental interactions. Exp Hematol; 35: 155-162.

23. Chauhan D, Li G, Podar K, Hideshima T, Shringarpure R, Catley L, Mitsiades C, Munshi N, Tai Y T, Suh N, Gribble G W, Honda T, Schlossman R, Richardson P, Sporn MB, and Anderson KC. (2004) The bortezomib/proteasome inhibitor ps-341 and triterpenoid cddo-im induce synergistic anti-multiple myeloma (mm) activity and overcome bortezomib resistance. Blood; 103:3158-3166.

24. Hideshima T, Mitsiades C, Tonon G, Richardson PG, Anderson KC. (2007) Understanding multiple myeloma pathogenesis in the bone marrow to identify new therapeutic targets. Nat Rev Cancer; 7: 585-598.

25. Colnot C, Fowlis D, Ripoche MA, Bouchaert I, and Poirier F. (1998) Embryonic implantation in galectin 1/galectin 3 double mutant mice. Dev Dyn; 211:306-313.

26. Colnot C, Ripoche A, Milon G, Montagutelli X, Crocker R, and Poirier F. (1998) Maintenance of granulocyte numbers during acute peritonitis is defective in galectin-3-null mutant mice. Immunology; 94:290-296.

27. Cumpstey I, Sundin A, Leffler H, and Nilsson J. (2005) C2-symmetrical thiodigalactoside bis-benzamido derivatives as high-affinity inhibitors of galectin-3: Efficient lectin inhibition through double arginine-arene interactions. Angew Chem Int Ed Engl; 44:5110-5112.

28. Dai Y, Landowski H, Rosen T, Dent P, and Grant S. (2002) Combined treatment with the checkpoint abrogator ucn-01 and mek1/2 inhibitors potently induces apoptosis in drug-sensitive and -resistant myeloma cells through an il-6-independent mechanism. Blood; 100: 3333-3343.

29. Dalton S, Durie G, Alberts S, Gerlach H, and Cress E. (1986) Characterization of a new drug-resistant human myeloma cell line that expresses p-glycoprotein. Cancer Res; 46:5125-5130.

30. Jarvis A, John M, and Leffler. (2001) N-terminally truncated galectin-3 for use in treating cancer. US Patent 6,770,622.

31. Dezorella N, Pevsner-Fischer M, Deutsch V, Kay S, Baron S, Stern R, Tavor S, Nagler A, Naparstek E, Zipori D, and Katz Z. (2009) Mesenchymal stromal cells revert multiple myeloma cells to less differentiated phenotype by the combined activities of adhesive interactions and interleukin-6. Exp Cell Res; 315:1904-1913.

32. Raz A, Lotan R.(1981) Lectin-like activities associated with human and murine neoplastic cells. Cancer Res; 41:3642-3647.

33. Dispenzieri A, Zhang L, Katzmann A, Snyder M, Blood E, Degoey R, Henderson K, Kyle A, Oken M, Bradwell R, and Greipp R. (2008) Appraisal of immunoglobulin free light chain as a marker of response. Blood; 111:4908-4915.

34. Engelhardt M, Kleber M, Udi J, Wasch R, Spencer A, Patriarca F, Knop S, Bruno B, Gramatzki M, Morabito F, Kropff M, Neri A, Sezer O, Hajek R, Bunjes D, Boccadoro M, Straka C, Cavo M, Polliack A, Einsele H, and Palumbo A. (2010) Consensus statement from european experts on the diagnosis, management, and treatment of multiple myeloma: From standard therapy to novel approaches. Leuk Lymphoma; 51(8):1424-43.

35. Eude-Le Parco I, Gendronneau G, Dang T, Delacour D, Thijssen VL, Edelmann W, Peuchmaur M, and Poirier F. (2009) Genetic assessment of the importance of galectin-3 in cancer initiation, progression, and dissemination in mice. Glycobiology; 19:68-75.

36. Fonseca R, and San Miguel J. Prognostic factors and staging in multiple myeloma. (2007) Hematol Oncol Clin North Am; 21:1115-1140.

37. Fosang J, Last K, Gardiner P, Jackson C, and Brown L. (1995) Development of a cleavage-site-specific monoclonal antibody for detecting metalloproteinase-derived aggrecan fragments: Detection of fragments in human synovial fluids. Biochem J. 310 (Pt1) :337-343.

38. Fosang J, Last K, Stanton H, Golub B, Little B, Brown L, and Jackson C. (2010) Neoepitope antibodies against mmp-cleaved and aggrecanase-cleaved aggrecan. Methods Mol Biol; 622: 312-347.

39. Friedrichs J, Manninen A, Muller J, and Helenius J. (2008) Galectin-3 regulates integrin alpha2beta1-mediated adhesion to collagen-i and -iv. J Biol Chem; 283:32264-32272.

40. Fuchida SI, Shimazaki C, Hirai H, Akamatsu S, Yamada N, Uchida R, Okano A, Okamoto M, Inaba T, and Taniwaki M. (2008) The effects of thalidomide on chemotactic migration of multiple myeloma cell lines. Int J Lab Hematol; 30:220-229.

41. Fukumori T, Kanayama O, and Raz A. (2007) The role of galectin-3 in cancer drug resistance. Drug Resist Update; 10:101-108.

42. Furtak V, Hatcher F, and Ochieng J. (2001) Galectin-3 mediates the endocytosis of beta-1 integrins by breast carcinoma cells. Biochem Biophys Res Commun; 289:845-850.

43. Ghazarian H, Idoni B, and Oppenheimer B. (2010) A glycobiology review: Carbohydrates, lectins and implications in cancer therapeutics. Acta Histochem; 13(3):236-47.

44. Granovsky M, Fata J, Pawling J, Muller J, Khokha R, and Dennis W. (2000) Suppression of tumor growth and metastasis in mgat5-deficient mice. Nat Med; 6:306-312.

45. Greenstein S, Krett NL, Kurosawa Y, Ma C, Chauhan D, Hideshima T, Anderson KC, and Rosen T. (2003) Characterization of the mm.1 human multiple myeloma (mm) cell lines: A model system to elucidate the characteristics, behavior, and signaling of steroid-sensitive and -resistant mm cells. Exp Hematol; 31:271-282.

46. Greipp R, San Miguel J, Durie G, Crowley J, Barlogie B, Blade J, Boccadoro M, Child A, Avet-Loiseau H, Kyle A, Lahuerta J, Ludwig H, Morgan G, Powles R, Shimizu K, Shustik C, Sonneveld P, Tosi P, Turesson I, and Westin J. (2005) International staging system for multiple myeloma. J Clin Oncol; 23:3412-3420.

47. Guess BW, Scholz C, Strum B, Lam Y, Johnson J, and JennrichI. (2003) Modified citrus pectin (mcp) increases the prostate-specific antigen doubling time in men with prostate cancer: A phase ii pilot study. Prostate Cancer Prostatic Dis; 6:301-304.

48. Guevremont M, Martel-Pelletier J, Boileau C, Liu T, Richard M, Fernandes C, Pelletier P, and Reboul P. (2004) Galectin-3 surface expression on human adult chondrocytes: A potential substrate for collagenase-3. Ann Rheum Dis; 3:636-643.

49. Hideshima T, Chauhan D, Shima Y, Raje N, Davies E, Tai T, Treon P, Lin B, Schlossman L, Richardson P, Muller G, Stirling I, and Anderson K. C. (2000) Thalidomide and its analogs overcome drug resistance of human multiple myeloma cells to conventional therapy. Blood; 96:2943-2950.

50. Hideshima T, Mitsiades C, Tonon G, Richardson PG, and Anderson KC. (2007) Understanding multiple myeloma pathogenesis in the BM to identify new therapeutic targets. Nat Rev Cancer; 7:585-598.

51 Chiriva-Internati M, Yu Y, Mirandola L, et al. (2010) Cancer testis antigen vaccination affords long-term protection in a murine model of ovarian cancer. PLoS One; 5:e10471.

52. Markowska AI, Liu FT, Panjwani N. (2010) Galectin-3 is an important mediator of VEGF- and bFGF-mediated angiogenic response. J Exp Med; 207:1981-1993.

53. Ochieng J, Fridman R, Nangia-Makker P, Kleiner DE, Liotta LA, et al. (1994). Galectin-3 is a novel substrate for human matrix metalloproteinases-2 and -9. Biochemistry; 33: 14109–14114.

54. Ochieng J, Green B, Evans S, James O, Warfield P (1998) Modulation of the biological functions of galectin-3 by matrix metalloproteinases. Biochem Biophys Acta; 1379: 97–106.

55. Mehul B, Bawumia S, Hughes RC (1995) Cross-linking of galectin 3, a galactose-binding protein of mammalian cells, by tissue-type transglutaminase. FEBS Lett; 360: 160–164.

56. Bleul CC, Fuhlbrigge RC, Casasnovas JM, Aiuti A, Springer TA (1996) A highly efficacious lymphocyte chemoattractant, stromal cell-derived factor 1 (SDF-1). J Exp Med; 184: 1101–1109.

57. Saraswati S, Block AS, Davidson MK, Rank RG, Mahadevan M, et al. (2011) Galectin-3 is a substrate for prostate specific antigen (PSA) in human seminal plasma. Prostate; 71: 197–208.

58 Akahani S, Nangia-Makker P, Inohara H, Kim HR, Raz A (1997) Galectin-3: a novel antiapoptotic molecule with a functional BH1 (NWGR) domain of Bcl-2 family. Cancer Res; 57: 5272–5276.

59. Moon BK, Lee YJ, Battle P, Jessup JM, Raz A, et al. (2001) Galectin-3 protects human breast carcinoma cells against nitric oxide- induced apoptosis: implication of galectin-3 function during metastasis. Am J Pathol; 159: 1055–1060.

60 Fukumori T, Kanayama HO, Raz A (2007) The role of galectin-3 in cancer drug resistance. Drug Resist Updat; 10: 101–108.

61. Zhao Q, Barclay M, Hilkens J, Guo X, Barrow H, et al. (2010) Interaction between circulating galectin-3 and cancer-associated MUC1 enhances tumour cell homotypic aggregation and prevents anoikis. Mol Cancer; 9: 154.

62. Mina-Osorio P, Soto-Cruz I, Ortega E (2007) A role for galectin-3 in CD13-mediated homotypic aggregation of monocytes. Biochem Biophys Res Commun; 353: 605–610.

63. Kuklinski S, Probstmeier R (1998) Homophilic binding properties of galectin-3: involvement of the carbohydrate recognition domain. J Neurochem; 70: 814–823.

64. Vande Broek I, Vanderkerken K, Van Camp B, Van Riet I (2008) Extravasation and homing mechanisms in multiple myeloma. Clin Exp Metastasis; 25: 325–334.

65. Plett PA, Frankovitz SM, Wolber FM, Abonour R, Orschell-Traycoff CM. (2002) Treatment of circulating CD34(+) cells with SDF-1alpha or anti-CXCR4 antibody enhances migration and NOD/SCID repopulating potential.Exp Hematol; 30:1061-9

66. Hsu DK, Chernyavsky AI, Chen HY, Yu L, Grando SA, et al. (2009) Endogenous galectin-3 is localized in membrane lipid rafts and regulates migration of dendritic cells. J Invest Dermatol; 129: 573–583.

67. Chauhan D, Li G, Podar K, Hideshima T, Neri P, et al. (2005) A novel carbohydrate-based therapeutic GCS-100 overcomes bortezomib resistance and enhances dexamethasone-induced apoptosis in multiple myeloma cells. Cancer Res 65: 8350–8358.

68. Medinger M, Fischer N, Tzankov A (2010) Vascular endothelial growth factor-related pathways in hemato-lymphoid malignancies. J Oncol; 729725 p.

69. Kiziltepe T, Anderson KC, Kutok JL, Jia L, Boucher KM, et al. (2010) JS-K has potent anti-angiogenic activity in vitro and inhibits tumour angiogenesis in a multiple myeloma model in vivo. J Pharm Pharmacol; 62: 145–151.

70 Anargyrou K, Dimopoulos MA, Sezer O, Terpos E (2008) Novel anti-myeloma agents and angiogenesis. Leuk Lymphoma; 49: 677–689.

71 Swelam WM, Al Tamimi DM (2010) Biological impact of vascular endothelial growth factor on vessel density and survival in multiple myeloma and plasmacytoma. Pathol Res Pract; 206: 753–759.

72 Mirandola L, Yu Y, Chui K, Jenkins MR, Cobos E, John CM, Chiriva-Internati M. (2011) Galectin-3C inhibits tumor growth and increases the anticancer activity of bortezomib in a murine model of human multiple myeloma. PLoS One;6 (7):e21811.

73. Chiriva-Internati M, Ferrari R, Yu Y, Hamrick C, Gagliano N, et al. (2008) AKAP-4: a novel cancer testis antigen for multiple myeloma. Br J Haematol; 140: 465–468.

74. Li WW, Hutnik M, Gehr G (2008) Antiangiogenesis in haematological malignancies. Br J Haematol; 143: 622–631.

75. Kotla V, Goel S, Nischal S, Heuck C, Vivek K, et al. (2009) Mechanism of action of lenalidomide in hematological malignancies. J Hematol Oncol; 2: 36.

76 Jeon S-B, Yoon HJ, Chang CY, Koh HS, Jeon S-H, et al. (2010) Galectin-3 Exerts Cytokine-Like Regulatory Actions through the JAK–STAT Pathway. The Journal of Immunology; 185: 7037–7046.

77. Hideshima T, Ikeda H, Chauhan D, Okawa Y, Raje N, et al. (2009) Bortezomib induces canonical nuclear factor-kappaB activation in multiple myeloma cells. Blood; 114: 1046–1052.

78. Greenstein S, Krett NL, Kurosawa Y, et al. (2003) Characterization of the MM.1 human multiple myeloma (MM) cell lines: a model system to elucidate the characteristics, behavior, and signaling of steroid-sensitive and -resistant MM cells. Exp Hematol; 31: 271-282.

79. Ishida BY, Bailey KR, Duncan KG, et al. (2004) Regulated expression of apolipoprotein E by human retinal pigment epithelial cells. J Lipid Res; 45:263-271.

80. Anderson KC. (2005). Lenalidomide and Thalidomide: Mechanisms of Action—Similarities and Differences. Seminars in Hematology; 42 (4 Suppl 4): S3–S8.

81. Chauhan D, Hideshima T, Anderson KC. (2005) Proteasome inhibition in multiple myeloma: therapeutic implication. Annu Rev Pharmacol Toxicol; 45:465-476.

82. Ciechanover A. (2005) Proteolysis: from the lysosome to ubiquitin and the proteasome. Nat Rev Mol Cell Biol; 6:79-687.

83. Richardson PG, Mitsiades C, Ghobrial I, Anderson K. (2006) Beyond single-agent bortezomib: combination regimens in relapsed multiple myeloma. Curr Opin Oncol; 18: 598-608.

84. Laubach JP, Mitsiades CS, Roccaro AM, Ghobrial IM, Anderson KC, Richardson PG. (2009) Clinical challenges associated with bortezomib therapy in multiple myeloma and Waldenstroms Macroglobulinemia. Leuk Lymphoma; 50: 694-702.

85. Shah JJ, Orlowski RZ. (2009) Proteasome inhibitors in the treatment of multiple myeloma. Leukemia; 23: 1964-1979.

86. John CM, Leffler H, Kahl-Knutsson B, Svensson I, Jarvis GA. (2003) Truncated galectin-3 inhibits tumor growth and metastasis in orthotopic nude mouse model of human breast cancer. Clin Cancer Res; 9: 2374-2383.

87. Nangia-Makker P, Honjo Y, Sarvis R, Akahani S, Hogan V, Pienta KJ, Raz A. (2000) Galectin-3 induces endothelial cell morphogenesis and angiogenesis. Am J Pathol; 156: 899-909.

88. Markowska AI, Liu FT, Panjwani N. (2010) Galectin-3 is an important mediator of VEGF- and bFGF-mediated angiogenic response. J Exp Med; 207: 1981-1993.

89. Byrd JC, Bresalier RS. (2004) Mucins and mucin binding proteins in colorectal cancer. Cancer Metastasis Rev; 23: 77-99.

90. Burton J, Mishina D, Cardillo T, Lew K, Rubin A, Goldenberg DM, Gold DV. (1999) Epithelial mucin-1 (MUC1) expression and MA5 anti-MUC1 monoclonal antibody targeting in multiple myeloma. Clin Cancer Res; 5: 3065s-3072s.

92. Kawano T, Ahmad R, Nogi H, Agata N, Anderson K, Kufe D. (2008) MUC1 oncoprotein promotes growth and survival of human multiple myeloma cells. Int J Oncol; 33: 153-159.

93. Yin L, Ahmad R, Kosugi M, Kufe T, Vasir B, Avigan D, Kharbanda S, Kufe D. (2010) Survival of human multiple myeloma cells is dependent on MUC1 C-terminal transmembrane subunit oncoprotein function. Mol Pharmacol; 78: 166-174.

94. Furtak V, Hatcher F, Ochieng J. (2001) Galectin-3 mediates the endocytosis of beta-1 integrins by breast carcinoma cells. Biochem Biophys Res Commun; 289: 845-850.

95. Rao SP, Wang Z, Zuberi RI, Sikora L, Bahaie NS, Zuraw BL, Liu FT, Sriramarao P. ((2007) Galectin-3 functions as an adhesion molecule to support eosinophil rolling and adhesion under conditions of flow. J Immunol; 179: 7800-7807.

96. Friedrichs J, Manninen A, Muller DJ, Helenius J. (2008) Galectin-3 regulates integrin alpha2beta1-mediated adhesion to collagen-I and -IV. J Biol Chem; 283: 32264-32272.

97. Saravanan C, Liu FT, Gipson IK, Panjwani N. (2009) Galectin-3 promotes lamellipodia formation in epithelial cells by interacting with complex N-glycans on alpha3beta1 integrin. J Cell Sci; 122: 3684-3693.

98. Paizi M, Manaster J, Quitt M, Spira G. (1991) High plasma fibronectin levels in multiple myeloma patients: possible mechanisms and clinical implications. Scand J Immunol; 34: 285-289.

99. Kurata M, Nakagawa Y, Yamamoto K, Suzuki K, Kitagawa M. (2008) Induction of integrin beta1 expression in bone marrow cells after chemotherapy correlates with the overexpression of lung resistance protein and poor outcome in patients with multiple myeloma. Am J Hematol; 83: 755-757.

100. Tai YT, Podar K, Catley L, Tseng YH, Akiyama M, Shringarpure R, Burger R, Hideshima T, Chauhan D, Mitsiades N, Richardson P, Munshi NC, Kahn CR, Mitsiades C, Anderson KC. (2003) Insulin-like growth factor-1 induces adhesion and migration in human multiple myeloma cells via activation of beta1-integrin and phosphatidylinositol 3'-kinase/AKT signaling. Cancer Res; 63: 5850-5858.

101. Parmo-Cabanas M, Bartolome RA, Wright N, Hidalgo A, Drager AM, Teixido J. (2004) Integrin alpha4beta1 involvement in stromal cell-derived factor-1alpha-promoted myeloma cell transendothelial migration and adhesion: role of cAMP and the actin cytoskeleton in adhesion. Exp Cell Res; 294: 571-580.

102. Chiriva-Internati M, Liu Y, Weidanz JA, Grizzi F, You H, Zhou W, Bumm K, Barlogie B, Mehta JL, Hermonat PL. (2003) Testing recombinant adeno-associated virus-gene loading of dendritic cells for generating potent cytotoxic T lymphocytes against a prototype self-antigen, multiple myeloma HM1.24. Blood; 102(9):3100-7.